An-Najah National University

Faculty of Graduate Studies

EFFECT OF PERIMETER BRICK-CONCRETE-STONE-MASONRY INFILL WALLS ON THE DEFLECTION AMPLIFICATION FACTOR (CD) FOR INTERMEDIATE MOMENT RESISTING FRAMES

By

Khalid Masarwa

Supervisors

Dr. Monther Dwaikat

Dr. Mohammad Samaaneh

This Thesis is Submitted in Partial Fulfillment of the Requirements for the Degree of Master of Structural Engineering, Faculty of Graduate Studies, An-Najah National University, Nablus, Palestine.

2024

EFFECT OF PERIMETER BRICK-CONCRETE-STONE-MASONRY INFILL WALLS ON THE DEFLECTION AMPLIFICATION FACTOR (CD) FOR INTERMEDIATE MOMENT RESISTING FRAMES

By

Khalid Jamal Abdelqader Masarwa

This Thesis was Defended Successfully on 12/06/2024 and approved by

Dr. Monther Dwaikat	
Supervisor	Signature
Dr. Mohammad Samaaneh	
Co-Supervisor	Signature
Dr. Abdulsamee Halahla	
External Examiner	Signature
Dr. Mahmud Dwaikat	
Internal Examiner	Signature

Dedication

This work is dedicated to:

The sake of Allah, my creator who gave me strength for everyday life.

My great teachers

My homeland Palestine, the symbol of sacrifice.

My parents, who have always loved me unconditionally this document is heartily dedicated to my mother.

My family, who help me to be who I am.

My uncles, especially my uncle Khalid.

My friends, who encouraged me.

All the people in my life who touch my heart, I dedicate this work.

Acknowledgment

I would like to thank my supervisors Dr. Monther Dwaikat and Dr. Mohammad Samaaneh who gave me the opportunity to undertake such great challenging work. I am grateful to them for their guidance, encouragement, understanding, and insightful support in the development process.

Last but not least I would like to sincere acknowledgment to all those whom I might have missed mentioning above who have helped me in this work.

May the almighty God richly bless all of you.

Declaration

I, the undersigned, declare that I submitted the thesis entitled:

EFFECT OF PERIMETER BRICK-CONCRETE-STONE-MASONRY INFILL WALLS ON THE DEFLECTION AMPLIFICATION FACTOR (CD) FOR INTERMEDIATE MOMENT RESISTING FRAMES

I declare that the work provided in this thesis, unless otherwise referenced, is the researcher's own work, and has not been submitted elsewhere for any other degree or qualification.

Student's Name: **Khalid Jamal Abdelqader Masarwa**

Signature: 

Date: **12/6/2024**

List of Contents

List of Tables

List of Figures

List of Appendices

EFFECT OF PERIMETER BRICK-CONCRETE-STONE-MASONRY INFILL WALLS ON THE DEFLECTION AMPLIFICATION FACTOR (CD) FOR INTERMEDIATE MOMENT RESISTING FRAMES

By
Khalid Masarwa
Supervisors
Dr. Monther Dwaikat
Dr. Mohammad Samaaneh

Abstract

Constructing of multi-story buildings using perimeter walls with stone cladding is very common in Palestine. The stone cladding provides an architectural aesthetic to the exterior facades of the buildings. The traditional method in Palestine to construct these walls is to fill the reinforced concrete frames with a three-layer wall. These layers are: brick, concrete, and stone. The walls may affect the behavior of the structure under an earthquake excitation. This results from their additional mass, lateral stiffness and strength that these walls add to the building. Neglecting the effect of these walls on the structural response can lead to a poor structural analysis prediction of the real structural behavior. Therefore, this study focuses on studying the effect of perimeter brick-concrete-stone-masonry (BCSM) infill walls on the deflection amplification factor (C_d) for intermediate moment resisting frames.

The research methodology started by designing 36 cases according to ASCE7-16 and ACI 318-14 codes. In every case, the building is designed as an intermediate moment resisting frame. Nonlinear static pushover analysis is performed to generate load-deflection curves for different parameters using SAP2000 computer program. The results are used to estimate the C_d-factor under the variation of the parameters.

In this study, it was found that the C_d-Factor is very sensitive to the presence of BCSM infill walls; it can lead to a significant change in the C_d-Factor compared to what is suggested by the ASCE7-16 code.

The results of this study showed that the increase of the BCSM infill walls opening ratio leads to a decrease in the C_d-Factor, and the increase of the BCSM infill walls length leads to a decrease in the C_d-Factor. Also, in this study, it was found that the C_d-Factor is not

fixed with varying the number of stories of a building. In other words, it is not true that the increase in the number of stories will always increase the C_d-Factor and vice versa.

Results were used to develop two simple formulas to estimate the C_d-Factor, and to help engineers in Palestine to estimate the C_d-Factor for buildings that have BCSM infill walls.

Keywords: Macro modeling; Fiber hinges; BCSM infill walls; C_d-Factor; R-Factor; Equivalent compression struts; Overstrength.

Chapter One
Introduction and Literature Review

1.1 Overview

In Palestine, buildings cladded with stone on their exterior walls are very common. The presence of these walls may affects the structural response of a building under an earthquake excitation since these walls add mass, stiffness, and strength to the building.

Seismological investigations and historical research indicate that there is a significant likelihood of damaging earthquakes in Palestine. Records show that Palestine has been subjected to an earthquake of 6.2 on Richter scale in 1927. Later in 2004, a 5.2 on the Richter scale earthquake has happened, but with no major damages that have been reported (Al-Dabbeek & El-Kelani, 2008).

Neglecting brick-concrete-stone-masonry (BCSM) infill walls from the structural analysis can lead to a poor structural analysis prediction between the structural analysis results and the real structural behavior. Such negligence, will affect the results of the fundamental period, the response modification factor (R) of the structure, the deflection amplification factor of the structure, and the distribution of seismic forces in the structure.

In recent years, Palestinians have become more conscious of the value of building structures to withstand earthquake forces. Additionally, the Palestinian Engineering Association created rules requiring structural engineers to conduct analyses and create earthquake-resistant building designs. The local common engineering design practice in Palestine is to neglect the additional lateral stiffness and the additional lateral strength that infill walls provide to the building and taking in consider only their mass as weight on the building.

Modeling of BCSM infill walls as a non-structural element is not clear yet to the structural engineers (Albayrak et al., 2017). This is as a result of the limited published researches in literature that study this type of walls. Adding to that, many parameters in infill walls will go into the infill wall structural properties such as: the length of the wall, layer thicknesses in the wall, opening ratio in the wall, type of wall material, contact length

between the wall and the surrounding frame, contact type, shear strength between the wall layers.

The goal of this study is to investigate the effect of typical BCSM infill walls in Palestine on the deflection amplification factor by creating macro models using the finite element program SAP2000. Material and geometrical nonlinearities will be included in the macro models.

A 36 RC building models that have perimeter BCSM infill walls were investigated in this study under several parameters. The selected parameters in this study to find the effect of BCSM infill walls on the C_d-Factors for RC intermediate moment resisting frames are: the length of the BCSM infill wall, the opening ratio in the BCSM infill wall, and the number of stories of the building.

Macro modeling for the BCSM infill walls was developed using an equivalent single diagonal compression strut. The properties of these struts were derived from a master thesis by Al-Hroub (2022). The capability of macro modeling to predict the behavior of RC frame with a BCSM infill wall was verified, then nonlinear static pushover analysis under several scenarios of parameters was performed to find the values of the deflection amplification factor.

After getting the results of the deflection amplification factor, two formulas were proposed to estimate the C_d-Factor. The first formula is to estimate the C_d-Factor if BCSM infill walls is considered in the design process in terms of its effect on the lateral stiffness and strength to the structure. In order to locally benefit from the study results, a second formula to estimate the C_d-Factor were proposed to help engineers in Palestine to get benefit of having BCSM infill walls in terms of lateral stiffness and strength, since the common design practice in Palestine only takes the effect of BCSM infill walls in terms of weight and mass.

1.2 Stone Cladding Methods in Palestine

As mentioned previously, buildings with stone cladding in Palestine are very common. Several methods were developed in Palestine to build walls with stone cladding (Halahla, 2019).

1.2.1 Method One (The Traditional Method)

In this method, stones arranged in rows (usually 3 rows). A thin layer of cement paste mortar is used to bind stone rows together and nearby stones are fastened to one another using an adhesive special material for stones. Also, stone wedges (wood or plastic) are installed from both faces of the stone to stabilize the pieces of stone before the concrete casting.

After constructing of the stone rows, shutter will be made to start pouring a concrete layer with compressive strength usually of 16.6 MPa (B 200) and thickness of about 12 cm to the level of the wanted built stone. The shutter could be wood or a10 cm hollow bricks that work as a permanent shutter as shown in Figure 1.1. This method results a BCSM infill wall. Figure 1.2 shows a section for the BCSM infill wall.

Figure 1.1

Method one shuttering types

a) Using 10 cm hollow brick as a permanent shutter b) Using wood shutter

Figure 1.2

BCSM infill wall section

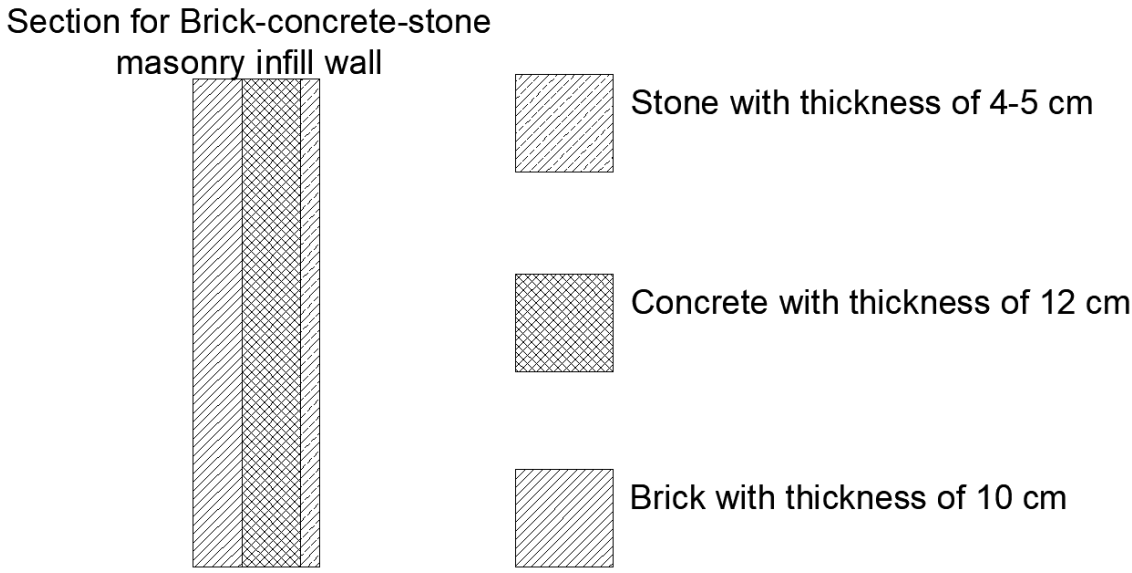

1.2.2 Method Two (Holding the stone layer to brick infill wall)

In this type of building, facades are mostly made of a brick layer that is positioned inside the boundaries of the frame, then a steel meshes of 6 mm diameter is installed to the brick layer. After that, a 6-10 cm space is made between the brick layer and the stone rows to pour concrete in it. Figure 1.3 shows an application of construction using method two.

Figure 1.3

An application of construction using method two

(Halahla, 2019).

1.2.3 Method Three

This method is very similar to method two, but the steel meshes are installed to a reinforced concrete wall not a brick-masonry infill wall. Figure 1.4 shows an application of construction using method three.

Figure 1.4

An application of construction using method three

Since Method One is the most famous method in Palestine (Al-Hroub, 2022; Halahla, 2019), this study will take care about this method only for a 10 cm hollow bricks as a permeant shutter for the scope of this study.

1.3 Methodology

Serious study is needed to address the uncertainties surrounding the performance of structures with infill walls; in order to improve the performance predictions of Palestinian local constructions against potential earthquakes. The fact of not having a local Palestinian code and adopting the American code seems to be incorrect since it is clearly obvious that the American construction methods are different from what is used to be applied in Palestine. Therefore, –and as an example- the suggested C_d-Factor for intermediate moment resisting frames (IMRF) in Palestine may not be conservative for the same moment resisting frames with BCSM infill walls.

The process of developing the research methodology began with a review of the relevant research literature. Following the literature study, construction and validation of the macro model was performed. After that, the main parameters in the parametric study were identified. Finally, macro models were developed using SAP2000 program and results were discussed using lumped plasticity (plastic hinges) approach.

Fiber hinges were used for beams and columns, and user-defined plastic hinges were used for the equivalent diagonal struts that represent the BCSM infill walls. Material and geometrical nonlinearities were included in all building models.

Unfortunately, there is a lack in literature for experiments that include frames with BCSM infills. Therefore, in this study, validation is carried out according to experiment that has been done by (Cavaleri et al., 2004) for a single-story single-bay RC bare frame. Also, validation is carried out according to a micro model that has been developed by Al-Hroub (2022) for single-story single-bay RC frame that include BCSM infill wall. After the macro modeling for all building models, nonlinear static pushover analysis under several scenarios of parameters was performed to find the values of the deflection amplification factor.

The behavior of RC buildings with BCSM infill walls is affected by many several parameters such as: openings, length of the BCSM infill wall, height of the BCSM infill wall, number of stories of the building, and other parameters. The effect of some of these parameters on the behavior of the RC buildings was studied. The study focused on three parameters. Those parameters are: the length of the BCSM infill wall, the opening ratio in the BCSM infill wall, and the number of stories in the building.

In this study, A 36 building models with perimetric BCSM infill walls were studied under different parameters, then the macro modeling results were used to develop two formulas to estimate the C_d- Factor.

1.4 Problem statement

The majority of seismic design codes in use today deal with the nonlinear response of a structure implicitly using design factors (such as R, C_d) to take into consideration the nonlinear behavior of the structure (such as the ASCE7-16 code). These factors make it possible for designers to use linear elastic force-based design. The ASCE7-16 Code not taking into consideration the presence of infill walls and its effect on the C_d-Factor and taking a single value for it for a specific type of a frames seems to be unjustified. Furthermore, the common engineering design practice ignores the presence of infill walls in the structural analysis models as they are considered a non-structural elements. Therefore, this study will focus on Method One of stone cladding to find its effect on the C_d-Factor for intermediate moment resisting frame buildings.

1.5 Research objective

The main objective of this study is to investigate the effect of perimeter BCSM infill walls on the deflection amplification factor for buildings with intermediate moment resisting frames.

This main objective will be achieved by satisfying the following objectives:

1. Verify the possibility of the macro models to describe the behavior of RC frame with BCSM infill wall.
2. Investigate the effect of BCSM infill walls on the deflection amplification factor.
3. Investigating the effect of the selected parameters on the C_d-Factor.
4. Developing a formula to estimate the C_d-Factor using the results of the parametric study.

1.6 Research scope and limitations

The scope of this research is to study the effect of perimeter BCSM infill walls on the deflection amplification factor for buildings with intermediate moment resisting frames in Palestine. The scope of this research is limited to BCSM infill walls that are being built in Palestine in term of materials, layers, and the stone cladding method. The research focused on Method One of stone cladding which was explained in Section 1.2.1.

1.7 Literature Review

Architectural aesthetics of exterior facades of the building can be made by stone cladding of the exterior perimeter walls. Neglecting these stone-cladded walls in the structural analysis and treating them as a non-structural elements could leads to inaccurate prediction of the seismic behavior of the building under an earthquake excitation. Studying masonry infill walls and their effect on the lateral behavior of a building has been an interest for researchers for more than sixty years (Halahla, 2019).

Numerical and experimental researches focused on studying the effect of infill walls on lateral stiffness, fundamental period, seismic design factors of buildings, and modeling methods. (Alguhane et al., 2016; Asteris et al., 2016; Huang et al., 2020; Shendkar et al., 2022). Many variables were studied by those researches such as: the presence of openings, length of the infill wall, and the material of the infill wall. Understanding the influence of infill walls on the deflection amplification factor is crucial for accurate

structural analysis and design particularly in seismic-prone regions where such factors play a significant role in determining the structural response to dynamic forces. In this chapter, literature related to frames with infill walls is reviewed and the results of this literature review are used to develop a research methodology and analysis methods.

1.7.1 Concrete Frames with Infill

According to FEMA 356-2000, "Concrete frames with infills are elements with complete gravity-load-carrying concrete frames infilled with masonry or concrete, constructed in such a way that the infill and the concrete frame interact when subjected to vertical and lateral loads. Isolated infills are infills isolated from the surrounding frame complying with the minimum gap requirements specified in Section 7.5.1." (FEMA356, 2000).

FEMA356 (2000) classifies infill walls into two types as following:

1. Masonry infill walls.
2. Concrete infill walls.

FEMA356-2000 states that in concrete infills, the concrete is likely to be of lower quality compared to that used in the frame and should be investigated separately. As mentioned in this Chapter, the common practice in Palestine uses Method One of stone cladding. Therefore, concrete infill walls are much known in Palestine.

1.7.2 Structural Roles of Infill Walls

The structural response to an earthquake excitation is significantly impacted by the existence of infill walls in the structure due to their additional stiffness, strength, and mass that they add to the building. "Infill walls in framed structures affect the dynamic characteristics of building such as stiffness, strength, and ductility of the entire structure and response to earthquakes" (Albayrak et al., 2017). The presence of infill walls in a structure can significantly impact its behavior (Sattar & Liel, 2010). Infill walls which are non-structural elements placed within the frames of a building, contribute to the overall stiffness and mass distribution of the structure. However, infill walls effect on the dynamic response of a structure can be complex. Infill walls can alter the dynamic characteristics of a structure by influencing factors such as natural frequencies, mode shapes, and the overall structural damping. The interaction between infill walls and the surrounding frame affects the stiffness and mass distribution which in turn can impacts

the response of a building to dynamic loads such as seismic or wind forces.

Ignoring the impact of infill walls in seismic locations is not prudent, because their presence will dramatically increase the lateral stiffness of the structure reducing its fundamental period and raising the seismic demands of the structure; as the reduction of the fundamental period of a structure increase the base shear demand for it (Asteris et al., 2016).

Previous studies using numerical methods and experimentations have shown the significance of infill walls in the structural dynamic analysis (De Angelis & Pecce, 2019; Manju, 2014). Although infill walls have a vital role on behavior of the structure, such walls are ignored in analyses for several reasons (Asteris et al., 2016):

1. Longer computational time.
2. Different responses of walls during an earthquake: useful at first but ineffective if walls are damaged.
3. Insufficient reliable data for the infill wall brittle materials behavior.
4. Common practice of construction effect.
5. The presence of openings in the infill diminishes their stiffness and influences their interaction with the frame, thereby modifying the overall dynamic characteristics of the structure.

It is important to notice that the specific effects of infill walls that they can affect the structure can vary based on several factors depend on the infill wall properties such as: the type of infill material, its geometry, the framing system of the structure, and others. Research studies, engineering literature, and publications on structural dynamics often delve into the complexities of how infill walls influence a structure's behavior.

1.7.3 Lateral Stiffness

Infill walls play a crucial role in influencing the overall stiffness of a structural frame. These walls typically constructed between the primary structural elements such as columns and beams, contribute significantly to the lateral load resistance of a building. Infill walls increase the lateral stiffness of the RC frame compared to bare frame (Sattar & Liel, 2010). The lateral stiffness of infill walls depends on many factors such as infill walls length, thickness, opening ratios, material properties, and the adjacent structural elements. When the thickness of the infill wall decreases, the lateral stiffness of the infill

wall will decrease since the wall becomes more susceptible to buckle (Abdelkareem et al., 2013). Also, the lateral stiffness of the infill wall will decrease when the infill wall length decrease. The presence of openings in an infill wall reduces its lateral stiffness (Jinya & Patel, 2014). The lateral stiffness of a brick wall decreases when the size of the surrounding columns increases (Qarout, 2018).

Abdel-Halim & Barakat (2003) experimentally studied the performance of concrete-backed stone masonry walls under cyclic loading by building 6 specimens at one-third scale. The study focused on the effect of several parameters such as: type of construction, the presence of dowels, and the presence of vertical loads. Their results showed that an increase in the applied vertical load resulted in a significant increase in both the lateral strength and stiffness of the tested samples.

Also, the effect of brick-concrete-stone masonry infill walls interface conditions on the RC frame lateral stiffness was studied experimentally by Al-Nimry (2014) under reversed cyclic loading by building 7 specimens (2 bearing wall models and 5 infilled frame models). The results showed that the use of dowel bars between infill wall and the surrounding RC frame increase the lateral stiffness around %50 compared to specimens with no dowel bars between the infill wall and the surrounding RC frame. Also, the study found that the increase in axial loading in the bearing wall specimens increases their lateral strength by %11, their energy dissipation capacity by %150, and their ductility by %53.

Many researches in the literature suggested the use of single equivalent compression struts with a specific width to represent the masonry walls stiffness such as: Mainstone & Weeks (1972) and Paulay & Priestley (1992) . Details on the equivalent compression strut are discussed in Sections 1.7.5.2 and 1.7.5.3.

1.7.4 Fundamental Period

Reliable estimation of the fundamental period is very important step to predict the response of a building under an earthquake excitation. Seismic response depends mainly on the natural period of the structure (Eleftheriadou et al., 2012). Also, Chopra (1995) showed that the inelastic displacement of the structure depends on both, the earthquake parameters and the fundamental period of the structure. Building Codes usually propose

multiple empirical formulas to estimate an approximate value for the fundamental period. Typically, these formulas are derived by applying regression analysis to data obtained from measured fundamental periods of existing buildings (Halahla, 2019). The formulas suggested by codes are developed to be conservative in the design approach. As a result, these code-prescribed formulas are intended to underestimate the fundamental period leading to an increase in the calculated base shear (Aninthaneni & Dhakal, 2016). In fact, many factors affect the fundamental period of a structure such as: mass of the structure, lateral stiffness of the structure, and construction practices. These formulas only take into account structural typology and the height of the structure (Chopra & Goel, 2000).

The natural time period for a single-degree-of-freedom structure can be computed according to equation (1.1).

$$Tn = 2\pi\sqrt{\frac{m}{k}} \tag{1.1}$$

Where:

m: the mass of the structure.
k: the lateral stiffness of the structure.

ASCE7-16 formulas for the calculation of the fundamental period

Section 12.8.2.1 of ASCE7-16 states that the approximate fundamental period (Ta) shall be calculated according to the following equation:

$$Ta = Ct\,(hn)^x \tag{1.2}$$

Where:

hn : it is the height of the structure.
Ct and x : are factors depend on the structural system, and they are determined from Table A1.1 in Appendix A.

Hence, the formula for reinforced concrete moment frames according to the ASCE7-16 code can be written as follows:

$$Ta = 0.0466\,(hn)^x \tag{1.3}$$

Alternatively, the ASCE7-16 code permits to calculate the approximate fundamental

period, in s, from equation 2.4 for structures not exceeding 12 stories above the base as defined in Section 11.2 (in ASCE7-16 code) where the seismic force-resisting system consists entirely of concrete or steel moment resisting frames and the average story height is at least 3 meters.

$$Ta = 0.1N \tag{1.4}$$

Where *N* is the number of stories above the base.
Also, for masonry or concrete shear wall structures, the ASCE7-16 code permits to calculate the approximate fundamental period from equation 1.5.

$$\text{Ta} = \frac{0.0019}{\sqrt{Cw}} hn \tag{1.5}$$

Where Cw is calculated from equation (1.6).

$$\text{Cw} = \frac{100}{Ag} \sum_{i=1}^{x} \left(\frac{hn}{hi}\right)^2 \frac{Ai}{1+0.83\left(\frac{hi}{Di}\right)^2} \tag{1.6}$$

Effects of parameters such as building height, bays number, infilled panels ratio to total number of panels and type of frame on the fundamental period of RC buildings were studied by Kose (2009). A new equation, has been proposed to predict the fundamental period of buildings. This equation, derived from the results of using multiple linear regression analysis, provides a more accurate estimate of fundamental periods compared to the equations suggested in UBC97 (Uniform Building Code 1997) and Eurocode 8 building codes.

According to a master thesis published in An-Najah University by Halahla (2019), showed that the influence of infill walls is a critical issue that needs to be taken into account because it directly affects both the fundamental period of the structure and it is regularity. Furthermore, the thesis included suggestions for improving earthquake design and evaluation for structures in Palestine by creating computations of the fundamental period for those with infill walls that have a particular stone cladding system.

1.7.5 Macro Modeling

1.7.5.1 Overview

In the literature, two approaches were adopted to model the infill walls; macro and micro modeling (Furtado et al., 2016). The micro modeling is more complex and very much time consuming, but it gives accurate and detailed results to represent the behavior of the structural elements. On the other hand, macro modeling is less time consuming, more convenient for engineers, and can give a proper representation of the problem (Li et al., 2019). The choice between macro and micro modeling depends on the required situation.

In this study, macro modeling has been used for the structural elements such as beams, columns, and the equivalent compression struts that represent the infill walls.

Also, in this study, the modeling of the BCSM infill walls was carried out in two stages: the first stage is to determine the width of an equivalent compression strut that represent the BCSM infill wall to represent the initial stiffness of the infill wall. The second stage is to assign a plastic hinge with specific properties such that this hinge will represent the nonlinear behavior of the BCSM infill wall in nonlinear structural analysis.

1.7.5.2 Equivalent compression strut width

Several research studies in the literature recommended to use single equivalent compression struts to represent the masonry infill walls (Polyakov, 1960). The method of equivalent strut for Macro-modeling is common and has been used (Alguhane et al., 2016). Macro modeling using the equivalent strut method (as shown in Figure B1.1 in Appendix B) focuses on computing basic parameters of these equivalent compression struts in their equivalent width, which affects both stiffness and strength. Simply, equivalent strut method calculates a width of a structural element in order to replace the infill wall panel by that structural element in such a way that represent the behavior of the infill wall panel (Abdelkareem et al., 2013). It was found that replacing these walls with an equivalent single compression strut as shown in Figure 1.5 is an appropriate approach to achieve the lateral stiffness of these walls.

The width of the compression strut depends on many factors such as the material of the infill wall, the geometry of the infill wall, the ratio of openings in the infill wall, and the stiffness of the surrounding frame (Qarout, 2018).

Figure 1.5

Equivalent frame with infill walls

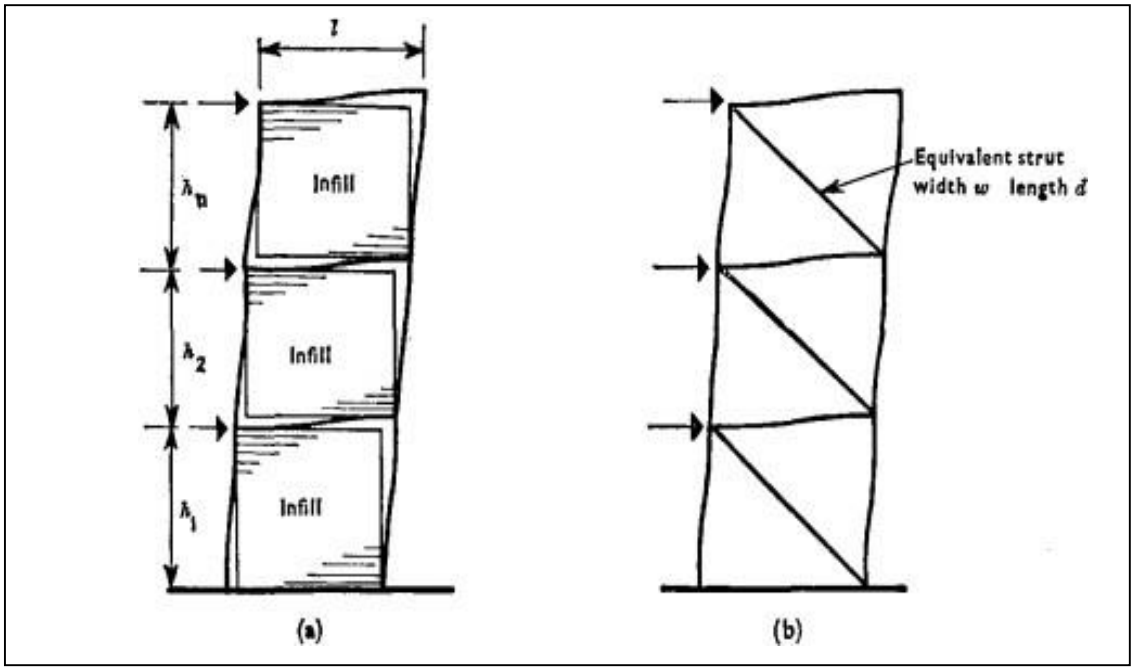

(Smith and Carter, 1969).

Several researches have developed a formula to compute the width of the equivalent compression strut. They include Mainstone (1971), Mainstone & Weeks (1972), and Paulay & Priestley (1992) . who developed equation (1.7), equation (1.8), and equation (1.9), respectively, to compute the width of the equivalent compression strut.

$$W = 0.16\, dinf\, (\lambda h\, hinf)^{-0.3} \tag{1.7}$$

$$W = 0.175\, dinf\, (\lambda h\, hinf)^{-0.4} \tag{1.8}$$

$$W = 0.25\, dinf \tag{1.9}$$

Where:

W: Width of the diagonal strut.

$dinf$: Length of the diagonal strut.

λh: Length of the horizontal contact between the diagonal strut and frame.

$hinf$: Height of infill wall.

Chrysostomou (1991) represented the masonry infill walls by 6 diagonal compression struts as shown in Figure B1.2 in Appendix B (3 struts in each direction).

According to FEMA356-2000 the ASCE/SEI 41-06 propose equation (1.10) to compute the equivalent width of strut.

$$W = 0.175\, dinf(\lambda 1 hinf)^{-0.4} \quad (1.10)$$

Where $\lambda 1$ can be calculated according to equation (1.11)

$$\lambda 1 = \left(\frac{Einf\ t\ sin2\theta}{4\ Ec\ Ic\ hinf}\right)^{0.25} \quad (1.11)$$

Figure B1.3 in Appendix B shows the parameters needed to compute the width of the diagonal strut.

Qarout (2018) proposed equation (1.12) to compute the width of the equivalent compression strut to represent the internal brick partition used in Palestine.

$$b = (L/8) - (Ac/1000) + 235 \quad (1.12)$$

Where:

b: is the width of the equivalent compression strut in (mm).
L: is the wall length in (mm).
Ac: is the gross sectional area of the column section in the surrounding frame in (mm^2).

The behavior of stone infill walls in Palestine for different stone cladding constructions methods was studied by Halahla (2019). The study focused on comparing several formulas for equivalent compression struts. The results showed that the strut width as computed using the National Building Code of Canada (NBCC) may be the best choice.

Most of the current publications like FEMA356-2000 propose calculations for stiffness for solid infills without giving a clear approach about the effect of openings on the effective compression strut width (Mondal & Jain, 2008).

New approach was developed by Ozturkoglu et al. (2017) to determine a stiffness reduction factors for infill walls that have openings. This reduction will affect the strut width which has been calculated to take into account the reduction of lateral stiffness of the infill walls caused by the presence of openings. The stiffness reduction factors for

partially infilled frames were computed considering the shape, the size and the position of the opening. Figure B1.4 in Appendix B shows an example for stiffness reduction factors calculated for a specific case for frame with bay length equal to 4 m, column dimension b=h=40 cm, and window opening at center.

A master thesis issued in Al-Najah University by Al-Hroub (2022) proposed a formula (equation (1.13)) to calculate the width of the equivalent compression strut to represent the lateral stiffness of the BCSM infill wall through design programs like SAP 2000, ETABS, and others, and to include the effect of lateral stiffness of BCSM infill walls in the seismic analysis. Also, the formula takes into account the effect of opening ratios that might be exist in the BCSM infill walls. Also, a comparison for 3 model with literature was done by this master thesis as shown in Figure B1.5 in Appendix B. Therefore, in this study, this formula has been adopted to calculate the equivalent diagonal compression strut width in all of the structural models.

$$Wa = (0.34 * L - 0.65 * t + 145)\, R \qquad (1.13)$$

Where:

Wa: It is the equivalent strut width of the stone wall(mm).
L: It is the length of the stone wall(mm).
t: It is the thickness of the plain concrete wall(mm).
R: it is the stiffness reduction factor calculated according to Figure B1.6 in Appendix B.

1.7.5.3 Constitutive Law for the Equivalent Compression Strut (the plastic hinge properties for the equivalent compression strut)

Reliable force-deformation parameters used to represent the nonlinear behavior of masonry infill walls are important to simulate the response of infilled reinforced concrete and steel structural systems under earthquake excitations. Infill walls significantly modify the seismic performance of buildings in term of stiffness, strength, and energy dissipation (Gaetani d'Aragona et al., 2021).

A database of 264 infilled frames experiments was collected by Huang et al. (2020) from existing literature, then the experimental data from a subset of 113 specimens was used in the calibration of the force-deformation parameters of the infill equivalent compression

strut. Table A1.2 in Appendix A shows the database sources that were assembled by Huang et al. (2020). Empirical formulas (shown in Table A1.3 in Appendix A) were proposed by Huang et al. (2020) for the backbone curve parameters to represent the nonlinear axial response of the infill equivalent compression struts after using the results from multivariate regression analysis. Figure B1.7 in Appendix B shows the backbone curve parameters that were derived by Huang et al. (2020).

A study about the influence of opening ratio and position in infill wall on constitutive law of equivalent compression strut was done by Öztürkoğlu & Ucar (2019), It was found that the force values of the force-deformation relationships decrease as opening ratio increases. Also, displacement values were not generally affected by the value of the opening ratio, or the position of it. Adding to that, openings upon the diagonal are more influential on the force-deformation relationships of the equivalent compression strut comparing it to other opening positions.

Therefore, in this study, the constitutive law for the equivalent compression strut for the BCSM infill walls was derived by calibrating the force-deformation parameters of the struts in such a way that a match with pushover curves that have been done by Al-Hroub (2022). This will be illustrated in Chapter 2.

1.7.6 Deflection Amplification Factor

Since the structure will pass the elastic stage under the seismic demand, nonlinear design is required. But nonlinear design (which take in consider the nonlinear behavior of the structural elements) is a complex process and very much time consuming. Therefore, the need for factors (like the C_d factor) that take in consider the nonlinearity effect of the structure under seismic excitation using linear elastic design is justified.

The deflection amplification factor, it "is the maximum nonlinear displacement during an earthquake (D_{max}), divided by the elastic displacement (D_s) calculated using reduced seismic design forces". (NEHRP, 2000).

The importance of calculating the maximum inelastic displacement for many several reasons, like the following:

1. Estimating story’s maximum drift.

2. Estimating the required distance of separation between structures to avoid the pounding issues.
3. Estimating the Deformation capacity for the structural members (displacement-based design).

Understanding the effect of infill walls on seismic design factors, such as the Response Modification Factor and the Deflection Amplification Factor is critical in structural engineering for earthquake-resistant design. Infill walls, although non-structural components exert a significant impact on the response of a building to seismic forces. The Response Modification Factor is a key parameter used to modify the elastic seismic forces and account for the energy dissipation and ductility provided by the structural system. Additionally, the deflection amplification factor (which is the concern in this study) helps to evaluate potential increases in lateral displacements due to the presence of infill walls. Figure 1.6 shows the general inelastic structural response.

Figure 1.6

General inelastic structural response

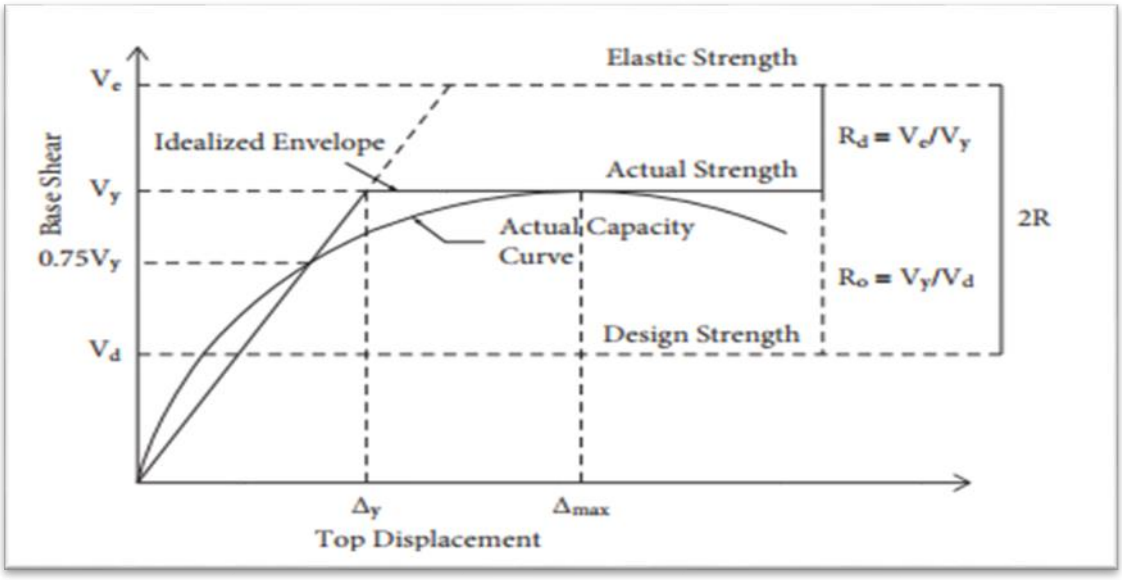

(Shendkar, 2022).

The deflection amplification factor can be calculated by multiplying the structural ductility factor (μs) with the overstrength factor (Ro) as expressed by (Uang, 1991) as follows:

$$C_d = \mu s \; x \; Ro = \frac{\Delta max}{\Delta y} \quad \frac{Vy}{Vd} \quad = \quad \frac{\Delta max}{\Delta y} \quad \frac{\Delta y}{\Delta d} \quad = \frac{\Delta max}{\Delta d} \qquad (1.14)$$

Where:

Δmax: it is maximum displacement corresponding to the peak base shear of the pushover curve (Park, 1988).

Δy: it is the yield displacement, calculated by reduced stiffness method (Park, 1988).

Δd: it is the displacement at the design base shear.

Vy: it is the ideal yield base shear.

Vd: it is the design base shear.

In this study, pushover curves are used to calculate the C_d-Factor for each building model. To do that, the yield and the maximum roof displacements shall be determined. The yield displacement of the roof is determined by the reduced stiffness method and the maximum displacement of the roof is corresponding to the peak base shear of the pushover curve (Park, 1988). After finding the yield and the maximum roof displacements, idealization of the building model pushover curve is done. Adding to that, to calculate the C_d-Factor for each building model the yield base shear (Vy) and the design base shear (Vd) shall be determined. The yield base shear is determined from the idealized pushover curve and the design base shear is calculated using the Equivalent Lateral Force Method as follows:

$$Vd = Cs * W \tag{1.15}$$

Where:

W: It is the effective seismic weight

Cs: It is the seismic response coefficient

The seismic response coefficient is determined according to ASCE7-16 Section 12.8.1.1 as follows:

$$Cs = \frac{S_{DS}}{R/Ie} \tag{1.16}$$

Where:

S_{DS}: it is the design, 5% damped, spectral response acceleration parameter at short periods as defined in Section 11.4.5 in the ASCE7-16 code.

R: it is the response modification factor determined from Table 12.2-1 in the ASCE7-16 code.

Ie: it is the importance factor determined from Table 1.5-2 in the ASCE7-16 code.

The value of Cs shall not exceed the following:

$$Cs = \frac{S_{D1}}{T\left(\frac{R}{Ie}\right)} \qquad \text{for } T \leq TL \tag{1.17}$$

$$Cs = \frac{S_{D1}}{T^2\left(\frac{R}{Ie}\right)} \qquad \text{for } T > TL \tag{1.18}$$

Also, Cs shall not be less than:

$$Cs = 0.044\, S_{DS}\, Ie \geq 0.01 \tag{1.19}$$

Adding to that, in Section 12.8.1.1 the ASCE7-16 states that for structures located where S1 is equal to or greater than 0.6g, Cs shall not be less than:

$$Cs = \frac{0.5S_1}{\left(\frac{R}{Ie}\right)} \tag{1.20}$$

Where:

S_1: it is the spectral acceleration parameter at a period of 1 sec.

S_{D1}: it is the design, 5% damped, spectral response acceleration parameter at a period of 1 s as defined in Section 11.4.5 in the ASCE7-16 code.

T: it is the fundamental period of the structure.

TL: it is the long-period transition period as defined in Section 11.4.6 in the ASCE7-16 code.

Deflection amplification factor can be taken from the IBC 2018/ASCE 7-16 code according to the seismic lateral force-resisting system as described in codes tables. Table A1.4 in Appendix A shows the C_d values for moment resisting frame system. The C_d value used for design in the direction under consideration shall not be lesser than the largest C_d value for any of the systems used in that direction.

The situation in the Euro code for the deflection amplification factor (symbolled by q)

depends on the prevailing failure mode by using a factor called kW, and by using a time-dependent response factor known as the behavior factor $q0$ as shown in equation (1.21).

$$q = q0 \times kW \tag{1.21}$$

Where:

q0: The main value for the response factor.

kW: express the prevailing failure mode (for moment resisting frames KW is taken to be 1).

The values of q0 can be taken from Table A1.5 in Appendix A.

Whereas, the Egyptian code adopts a 0.75 of the response reduction factor to compute the C_d value, and the Egyptian code talked about the R-values in Chapter 8 [Loads and forces on structural and nonstructural systems]. The Egyptian code states that the R values for RC moment resisting frames based on the level of ductility of the moment resisting frame as shown in Table A1.6 in Appendix A.

Analytical study was done by Samimifar et al. (2015) about the seismic responses of several reinforced concrete frames subjected to earthquake records. The study recommended a minimum value of 1.0 for the C_d/R ratio in order to estimate maximum inelastic drifts. Also, the observed RC models generally exhibited a slight increase in the ratio of inelastic to elastic displacement as one moved along the structural height.

Also, a study by Shendkar et al. (2022) for a four-story and three-dimensional reinforced concrete building with various infill wall patterns that take into account the openings presence in the infill walls found that the R values of all the RC infilled frames decrease as long as the compressive strength of the masonry infill decreases. Also, it was found that the R values of bare frames are lower than the comparable values suggested in the BIS code. In addition, the deflection amplification factors of the RC frames are underestimated by the National Earthquake Hazards Reduction Program provisions based on the evaluated deflection amplification factors of the RC frames under his study. Table 1.1 shows the comparison of seismic design factors for all structural models that were built in the study.

Table 1.1

Comparison of seismic design factors structural models

Frame system	Ductility reduction factor (R_d)			Response reduction factor (R)			Ductility (μ)			Overstrength factor (R_O)			Deflection amplification factor ($C_d = \mu \times R_o$)			Deflection factor ($DF = \mu/R_d = C_d/2R$)		
	Compressive strength of infill (MPa)			Compressive strength of infill (MPa)			Compressive strength of infill (MPa)			Compressive strength of infill (MPa)			Compressive strength of infill (MPa)			Compressive strength of infill (MPa)		
	5	4	3	5	4	3	5	4	3	5	4	3	5	4	3	5	4	3
Full RC infilled frame in *X* axis	1.15	1.13	1.15	5.86	5.36	5.16	1.16	1.14	1.17	10.19	9.5	8.98	11.82	10.83	10.50	1.01	1.01	1.02
Full RC infilled frame in *Y* axis	1.15	1.13	1.15	5.86	5.48	5.17	1.16	1.14	1.17	10.20	9.7	9.0	11.83	11.05	10.53	1.01	1.01	1.02
Corner infill at ground story RC infilled frame in *X* axis	1.80	1.90	1.32	4.27	4.26	2.93	2.12	2.31	1.37	4.75	4.49	4.45	10.07	10.37	6.09	1.18	1.22	1.04
Corner infill at ground story RC infilled frame in *Y* axis	1.80	1.28	1.30	4.27	3.05	2.94	2.13	1.32	1.34	4.75	4.77	4.53	10.11	6.29	6.07	1.18	1.03	1.03
Open ground story RC infilled frame in *X* axis	1.79	1.64	1.75	1.94	1.78	1.89	1.94	1.85	1.75	2.17	2.17	2.17	4.20	4.01	3.79	1.08	1.13	1.00
Open ground story RC infilled frame in *Y* axis	1.71	1.65	1.89	1.85	1.78	2.04	1.97	1.87	1.89	2.16	2.16	2.16	4.25	4.03	4.08	1.15	1.13	1.00
Bare frame in *X* axis	1.64	1.64	1.64	1.43	1.43	1.43	1.64	1.64	1.64	1.75	1.75	1.75	2.87	2.87	2.87	1.00	1.00	1.00
Bare frame in *Y* axis	1.63	1.63	1.63	1.43	1.43	1.43	1.63	1.63	1.63	1.76	1.76	1.76	2.86	2.86	2.86	1.00	1.00	1.00

Built by Shendkar et al. (2022).

Chapter Two
Macro Modeling and Case Study Analysis

2.1 Introduction

Infill walls modeling has been an interest to many researchers for several years. Degree of complexity and the analysis methods is not the same; whereas some modeling methods deal with the components of the infill walls, others substitute the infill wall by an equivalent compression strut. In this study, an equivalent compression strut is found to be the most applicable method for BCSM infill walls modeling. Therefore, the properties of the struts that will be used in this study derived from a master thesis that has been issued in Al-Najah University by Al-Hroub (2022).

As mentioned in Chapter 1 (Section 1.7.5.1), modeling of the BCSM infill walls is carried out in two stages: the first stage is to find the width of an equivalent compression strut that represent the BCSM infill wall to represent the lateral stiffness of the infill wall, the second stage is to assign a plastic hinge with specific properties to that equivalent compression strut such that this hinge will represent the nonlinear behavior of the BCSM infill wall in nonlinear structural analysis. The first stage is done by using equation (1.13) suggested by Al-Hroub (2022) to find the equivalent compression strut width, and the second stage is done by calibrating the force-deformation parameters for plastic hinges of the struts until a visual match is obtained with the required pushover curves presented in Al-Hroub (2022) master thesis for 2D frames. The buildings in this study are designed according to the ASCE7-16 and ACI 318-14 codes, then fiber plastic hinges are assigned to the columns and the beams.

After structural modeling for all buildings, nonlinear static pushover analysis is done to find the effect of BCSM infill walls on the deflection amplification factor for intermediate moment resisting frames.

2.2 Macro Modeling of BCSM Infill Walls

The first stage to represent the BCSM infill wall is to find the width of an equivalent compression strut that represent the BCSM infill wall to represent the lateral stiffness of that infill wall, in this study, this is done by using equation (1.13) suggested by Al-Hroub (2022). Equation (1.13) implicitly assumes that the bricks have a modulus of elasticity of

6800 MPa. Therefore, it will be assumed that the infill wall consists of one layer of concrete with thickness of 162.6 mm for all strut models using the transformation section method.

In this study, a 12 equivalent compression strut models are used for the parametric study, these models represent BCSM infill walls with lengths of 7 m, 5.5 m, and 4 m, and with opening ratios of %0, %15, %30, and %60.

Table 2.1 shows the equivalent compression strut width for walls with multiple lengths and opening ratios that will be used in this study.

Table 2.1

Equivalent compression strut width for walls with multiple lengths and opening ratios

Infill Wall Length (mm)	Infill Wall Opening Ratio (%)	Equivalent Compression Strut Width (mm)
7000	0	2420
7000	15	1694
7000	30	968
7000	60	424
5500	0	1910
5500	15	1337
5500	30	764
5500	60	335
4000	0	1400
4000	15	980
4000	30	560
4000	60	249

After obtaining the dimensions of the equivalent compression struts, the second stage to represent the BCSM infill wall comes. The second stage is to assign axial plastic hinges to those equivalent compression struts with a specific force-deformation parameters.

The force-deformation parameters (as shown in Figure B2.1 in Appendix B) for each equivalent compression strut were derived from pushover curves that were obtained by Al-Hroub (2022). This is done using SAP2000 program by modeling 2D frames that have been developed by Al-Hroub (2022) then calibrating the force-deformation parameters for the struts' plastic hinges until a visual match is obtained with the required pushover curves presented in Al-Hroub (2022) for the 2D frames.

Figure B2.2 in Appendix B shows an example for the visual match for RC frame with BCSM infill wall with length of 5.5 m, and opening ratio of %30.

Table 2.2 shows the force-deformation parameters for the 12 equivalent compression strut models that will be used in this study.

Table 2.2

Force-deformation parameters for walls with multiple lengths and opening ratios

Infill Wall Length (m)	Infill Wall Opening Ratio (%)	F1 (kN)	F2 (kN)	F3 (kN)	F4 (kN)	U1 (mm)	U2 (mm)	U3 (mm)	U4 (mm)
4	0	1340	1916.2	1996.6	1768.8	1.56	2.56	5.56	8.56
4	15	760	1064	1102	722	1.26	1.96	4.36	9.86
4	30	600	798	798	720	1.59	2.29	6.09	9.99
4	60	300	414	450	360	1.78	2.78	5.76	9.88
5.5	0	1730	2300.9	2525.8	2595	1.84	2.64	5.04	7.1
5.5	15	992	1349.12	1408.64	1190.4	1.5	2	4.1	5.9
5.5	30	620	886.6	998.2	1397.48	1.65	2.65	5.15	6.95
5.5	60	350	507.5	574	525	2.12	3.22	6.12	7.02
7	0	1912	2715.04	3154.8	2925.36	1.94	2.84	5.44	7.54
7	15	1335	1802.25	1909.05	1815.6	1.76	2.46	3.76	5.46
7	30	870	1122.3	1226.7	1122.3	1.84	2.44	3.64	6.14
7	60	420	525	634.2	609	2.03	2.63	5.83	6.38

2.3 Macro Modeling of Columns and Beams

Macro modeling of columns and beams is also done in two stages in this study, the first stage is to design the buildings according to the ASCE7-16 and ACI 318-14 codes, then the second stage is to assign fiber plastic hinges to columns and beams. Macro modeling of columns and beams using fiber hinges is a method employed in structural engineering to simulate the behavior of these structural elements under various loading conditions. In this approach, the complex material behavior of reinforced concrete is simplified by representing the concrete and reinforcement as a network of discrete fibers, each with its mechanical properties. These fiber hinges allow for a more accurate prediction of the structural response, including flexural and axial behavior, as well as the interaction between columns and beams. By incorporating fiber hinges into the macro model, engineers can gain valuable insights into the structural performance, enabling them to design safer and more efficient buildings.

In this study, the stress-strain behavior for the concrete material fibers is according to Mander stress-strain model for confined and unconfined concrete, and the stress-strain behavior for the rebar material fibers is according to park. These two models are available in SAP2000 program.

SAP2000 program provides a feature called section designer, this feature allows the users to draw sections with composite materials (for example column with rebars) and define a unique stress-strain curve for each material, then the program automatically will calculate properties related to that section such as the moment-curvature curve, interaction surface of the section, and the plastic hinge properties for that section.

Figure B2.3 in Appendix B shows a reinforced concrete column section that has been drawn using the section designer, the yellow area represents the cover of the column which is unconfined concrete, the cyan area represents the core of the column which is confined concrete, and the black area represents the rebars of the column. The column dimensions are 500x500 mm, the concrete compressive strength 28 MPa, the rebars diameter is 18 mm, ties diameter is 10 mm, number of ties is four in X and Y directions, and the yield strength for rebars and ties is 414 MPa.

Figure B2.4, Figure B2.5, and Figure B2.6 in Appendix B show the stress-strain curves for the materials of the column, Figure B2.4 shows the stress-strain curve for the unconfined concrete of the column, Figure B2.5 shows the stress-strain curve for the confined concrete of the column, and Figure B2.6 shows the stress-strain curve for rebars of the column.

2.4 Case Study Analysis

To study the BCSM infill walls on the deflection amplification factor for intermediate moment resisting frames, a case study building is assumed to compare the results of the C_d-Factor with the provided in building codes. This is done by modeling the case study building, and performing a nonlinear static pushover analysis as will be illustrated in the following sections.

2.4.1 Case Study Description

In this subsection, assumed case study for a building will be described. The description will include: the model description, the site seismicity, the structural system for the model, materials of the model, and vertical loads of the model.

2.4.1.1 Model Description

The assumed building is a five-story RC-IMRF where all floors consist of stories with a height of 3.12 m and a total building height of 15.6 m. The building has a square shape with three bays in both the X and the Y directions. All of the bays have a length of 5.5 m. BCSM infill walls with length of 5.5 m and with opening ratio of %30 were assumed to represent the perimeter facades. These BCSM infill walls is represented by using equivalent compression struts as has been mentioned in Section 2.2. modeling is done using SAP2000 program.

in Appendix B, Figure B2.7 shows the 3D view of the building, Figure B2.8 shows the 2D view of the building, and Figure B2.9 shows the columns distribution.

2.4.1.2 Site Seismicity

The building is assumed to be in Nablus city where the spectral acceleration parameter at short periods (Ss) is equal to 0.75g and the spectral acceleration parameter at a period of 1 sec ($S1$) is equal to 0.15. Also, the soil of the site is assumed as rock soil according to the classification of ASCE 7-16. Rock soil comes as [B] among soil classifications (ASCE7-16, 2016), see Table A2.5 in Appendix A.

2.4.1.3 Structural System for The Model

Frames are assumed to resist both lateral and gravity loads. The selected building consists of two- way-solid slab with beams with slab thickness of 20 cm. The frames are assumed to be intermediate moment resisting frames. The effect of BCSM infill walls on the fundamental period of the building is considered for the frames design. Beams are distributed in both principal directions. All columns are square columns of the same dimensions (50 cm X 50 cm) and the same reinforcement. The connection between the columns and the foundations is assumed to be fixed.

Table A2.1 in Appendix A shows the characteristic of the structural elements.

2.4.1.4 Materials of The Model

The selected building is made of reinforced concrete. The compressive strength of concrete (f'c) is different for slab, beams, struts, and columns. Concrete unit weight is 25 kN/m^3. The steel type is ASTM A615 Grade 60. Equation (2.1) shows an empirical

formula to calculate the modulus of elasticity of concrete (ACI 318-14, 2014). Table A2.2 in Appendix A shows the properties of the materials used.

$$E = 4700\sqrt{f'c} \quad \text{(in MPa)} \tag{2.1}$$

Where:

E: modulus of elasticity of concrete (MPa).

$f'c$: concrete 28-day cylindrical compressive strength MPa.

2.4.1.5 Vertical Loads of The Model

The building is assumed to be a residential building. Therefore, live loads were taken according to ASCE7-16 standard. A value of 3 kN/m^2 were adopted for the live loads, A value of 4 kN/m^2 were adopted for the superimposed dead load calculated based on typical finishes in Palestine, and a value of 16.5 kN/m were adopted for the superimposed dead load on the perimeter beams.

Table A2.3 in Appendix A shows the derivation of the number 16.5 kN/m, and Table A2.4 in Appendix A shows the summary of the adopted vertical loads.

2.4.2 Pushover Analysis

In order to perform pushover analysis, the nonlinear behavior of the elements has to be defined. SAP2000 is a powerful tool to capture the nonlinear behavior of a structure. It is simple and user-friendly to capture the plastic behavior through concentrated and distributed plasticity approaches. A new feature developed in SAP2000 version 2025 allows users to use distributed plasticity for frame members. Therefore, in this study, a concentrated plasticity (or lumped plasticity) approach will be used for the equivalent compression struts by assigning a user-defined plastic hinges to those equivalent compression struts. A distributed plasticity approach will be used for beams and columns by assigning a fiber plastic hinges to those beams and columns.

2.4.2.1 Definition of Plastic Hinges

Several methods are available in SAP2000 to define plastic hinges. As mentioned in Section 2.3, fiber plastic hinges for columns and beams are defined automatically using the section designer feature and the user-defined plastic hinges for the struts (which represent the BCSM infill walls) are defined according to Table 2.2.

For the case study building, fiber plastic hinges are defined to be fiber P-M2-M3 as shown in Figure B2.10 in Appendix B. in Appendix B, Figure B2.11 shows the definition data of the fibers for the beams, Figure B2.12 shows the definition data of the fibers for the columns, and Figure B2.13 shows the axial plastic hinge definition for the equivalent compression strut.

Paulay and Priestley (1992) have suggested the following formula for the estimation of the plastic hinge length.

$$Lp = 0.08z + 0.022\, db\, fy \tag{2.2}$$

Where:

z: is the distance of critical section to point of contraflexure.

db: is the longitudinal rebars diameter.

fy: is the yield strength for the rebars.

They suggested that, for typical beam or column proportion, the above formula results in values of $Lp \approx 0.5h$, where h is the section depth. Therefore, Lp = 0.5*0.5 = 0.25 m will be assumed beams and columns since the section depth for beams and columns is 50 cm. Figure B2.14 in Appendix B shows the assumed plastic hinge length for beams and columns.

2.4.2.2 Lateral Load Pattern

To perform pushover analysis, the lateral load pattern has to be related to the fundamental mode shape in order to be close as possible to the response of the building under an expected earthquake. Table A2.6 in Appendix A below shows the modal shape vector for

the translational fundamental mode in X-direction which are normalized by the top floor displacement.

2.4.2.3 Load Cases Definition for Pushover Analysis

The lateral load pattern mentioned in the previous section has to be defined in the pushover load case, but this case shall begin after the end of a gravity load case which has to be defined also. The gravity load case includes the dead load and a %25 of the live load (%25 of the live load is assumed to act on the building). Also, P-Δ analysis is included in the pushover load case definition. The pushover analysis is displacement controlled; the monitored displacement is the roof floor displacement. The pushover analysis stops at a roof floor displacement corresponding to the maximum base shear. In Appendix B, Figures B3.15, and B3.16 show the gravity load case definition and the pushover load case definition, respectively.

2.4.2.4 Pushover Curve for the Model

After defining the pushover load case for the model (Section 2.4.2.3), pushover analysis is done. Figure 2.1 shows the resulted base shear vs. roof displacement for the model.

Figure 2.1

Base shear vs. roof displacement for the model

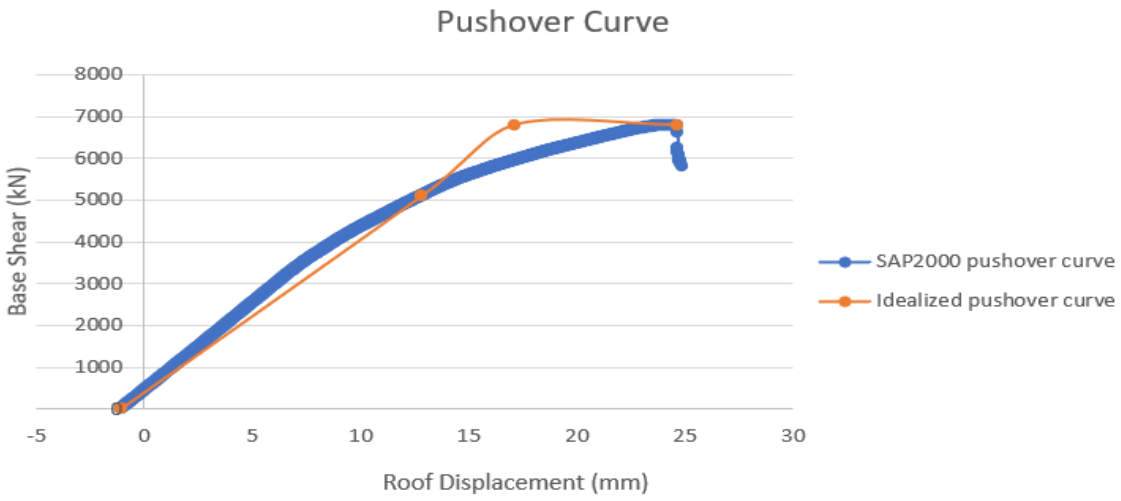

From the pushover curve, the C_d-Factor can be calculated according to equation (2.14) as following:

$$C_d = \mu s \; x \; Ro = \frac{\Delta max}{\Delta y} \quad \frac{Vy}{Vd} \quad = \quad \frac{24.63}{17.1} \quad \frac{6799}{1035} \quad = 1.44 * 6.57 = 9.46$$

According to the ASCE7-16 code, the Cd-Factor for intermediate moment resisting frames is 4.5. a very significant difference in the C_d-Factor has been observed for this model. In the next chapter, a parametric study is conducted to evaluate the effect of BCSM infill walls on the C_d-Factor for intermediate moment resisting frames.

2.5 Validation

In structural analysis, model validation plays a crucial role in ensuring the accuracy and reliability of computational models used to simulate the behavior of physical structures under various loading conditions. Structural analysis involves predicting the response of a structure to applied loads, such as forces, moments. Model validation in structural analysis typically involves comparing the predictions of a computational model (the finite element model) with experimental measurements or analytical solutions obtained from established theories.

The goal is to verify that the model accurately represents the real-world behavior of the structure. Unfortunately, there is a lack in literature for experiments that include frames with Brick-Concrete-Stone infills. Al-Nimry (2014) conducted an experiment for BCSM infill walls, but for one-third scale specimens which cannot be used for validation, since the validation methodology will not be consistent with the way that the plastic hinge properties were derived in Section 2.2. Therefore, in this study, validation is carried out according to experiment that has been done by (Cavaleri et al., 2004) for a single-story single-bay RC bare frame. Also, validation is carried out according to a micro model that has been developed by Al-Hroub (2022) for single-story single-bay RC frame that include BCSM infill wall with a length of 4 m and %0 opening ratio (this micro model is not the same micro model which the force-deformation parameters for the equivalent compression strut were derived in Section 2.2 for BCSM infill wall with a length of 4 m and %0 opening ratio; the micro model has a concrete thickness of 15 cm instead of 12 cm).

- **Experiment Data from** (Cavaleri et al., 2004)

1) The span of the frame is 1800mm c/c, and the story height is 1800mm c/c.
2) The reinforcement detailing and the geometrical properties of the RC frame is shown in Figure B2.17 in Appendix B.
3) Material properties:

- Concrete compressive strength is 30 MPa.
- The yield strength of steel is 434 MPa and the modulus of elasticity of steel is 190000 MPa.

a) Manual calculations

Using section designer in SAP2000:

The yielding moment for the beam (Myb) = 24.35 kN.m.

The yielding moment for the column (Myc) = 15.5 kN.m.

The curvature of the column at yield (Øyc) = 0.00818 1/m.

The curvature of the beam at column yielding (Øb@ Øyc) = 0.00455 1/m.

The ultimate moment for the beam (Mub) = 35.21 kN.m.

The ultimate moment for the column (Muc) = 22.43 kN.m.

Therefore, the expected collapse mechanism is a sway mechanism.

Using the upper bound theorem:

$\sum$ External work = $\sum$ Internal work

$1.8*F_{Collapse} = 4*22.43$

$F_{Collapse} = 49.84$ kN

Assuming the bending moment inflection point is in the middle of the columns, Figure B2.18 in Appendix B shows the bending moments on the frame elements due to 1-unit load and Figure B2.19 in Appendix B shows the curvature of the frame elements when the columns reach yielding.

Using the principle of the virtual work:

The yielding displacement (Δy) of the frame = 4(0.5*0.9*0.44* (0.00818/0.9)*(2/3)*0.9) + 2(0.5*0.9*0.44*(0.00455/0.9)*(2/3)*0.9) = $5.547 * 10^{-3}$ m = 5.547 mm

b) SAP2000 Pushover Analysis

Macro modeling is done for the RC frame according to the experiment, then pushover analysis is carried out. The pushover analysis is stopped until a roof displacement of 18.5 mm as to what has been done for the experiment. Figure B2.20 in Appendix B shows a comparison between the pushover curves for experiment, SAP 2000, and manual pushover curves.

- **Micro Model Data from** (Al-Hroub, 2022)

1) The span of the frame is 4000mm c/c, and the story height is 3120mm c/c.
2) The reinforcement detailing and the geometrical properties of the RC frame is shown in Table A2.7 in Appendix A.
3) Material properties:

- Concrete compressive strength is 24 MPa for the column and the beam.
- Concrete compressive strength is 16.6 MPa for the concrete infill (the thickness of the concrete infill is 15 cm).
- Brick compressive strength is 6.8 MPa.
- The yield strength of steel is 420 MPa and the modulus of elasticity of steel is 200000 MPa.

4) Axial load on each column is 850 kN.

SAP2000 Pushover Analysis

Macro modeling is done for the RC frame according to the experiment. The force-deformation parameters for the equivalent compression strut are derived from Table 2.2 as shown below. After that pushover analysis is carried out.

Infill Wall Length (m)	Infill Wall Opening Ratio (%)	F1 (Kn)	F2 (Kn)	F3 (Kn)	F4 (Kn)	U1 (mm)	U2 (mm)	U3 (mm)	U4 (mm)
4	0	1340	1916.2	1996.6	1768.8	1.56	2.56	5.56	8.56

Figure B2.21 in Appendix B shows a comparison between pushover curves for Al-Hroub (2022) micro model and SAP 2000 pushover curves.

In Appendix B, Figure B2.20 and Figure B2.21 show a good correlation between the results of the pushover analysis of the tested frames and the analysis results of the

developed macro models. Therefore, the infill wall model and their associated material properties can be used in this study.

Chapter Three

Parametric study and C_d-Factors Estimation for Prototype Buildings

3.1 Introduction

To study the effect of BCSM infill walls on the C_d-Factors for RC intermediate moment resisting frames, several parameters is included in this study to develop prototype building models. These parameters are: the length of the BCSM infill wall, the opening ratio in the BCSM infill wall, and the number of stories of the building.

In this study, a 36 building models were analyzed and designed according to ASCE7-16 and ACI 318-14 codes, then nonlinear static pushover analysis was done for these building models in order to generate load-deflection curves for several scenarios of the parameters. This chapter shows the building models, the corresponding pushover curves for these building models under several scenarios of the parameters, and shows how these pushover curves are used to calculate the C_d-Factors.

3.2 Parametric Study

As to what has been mentioned in Chapter 1, the presence of infill walls affects the behavior of an RC structure. This is due to the additional stiffness and strength that these walls add to a structure (Dautaj et al., 2018). Several parameters affect the behavior of an RC structure such as: the length of the infill wall, the material of the infill wall, the presence of openings, axial load on the columns, and other parameters (AbdelRahman & Galal, 2022). As mentioned in Section 3.1, the selected parameters in this study to find the effect of BCSM infill walls on the C_d-Factors for RC intermediate moment resisting frames are: the length of the BCSM infill wall, the opening ratio in the BCSM infill wall, and the number of stories of the building. The selected lengths of the BCSM infill walls are: 4m, 5.5m, and 7 m as these lengths represent the typical center to center distances between columns in Palestine. The selected opening ratios in the BCSM infill walls are: %0, %15, %30, and %60 since openings affect the lateral stiffness and strength of the RC frames (Akhoundi et al., 2016). The number of stories selected for the buildings are: 5, 8, and 11 since the number of stories for a building affects the fundamental period of the building and the lateral force distribution. Table A3.1 in Appendix A shows the properties of the 36 building models that will be used in this study.

3.3 Analysis Methodology

To estimate the C_d-Factors for the 36 building models in this study, the process started by designing all of the 36 building models according to ASCE7-16 and ACI 318-14 codes. Every building model is designed as an intermediate moment resisting frame. ASCE7-16 code specify value of R=5 and this value was used in the design process. Also, ACI318-14 code requirements for reinforcement detailing is followed. The effect of the BCSM infill walls on the fundamental period of the structures was taken into account in the design process.

After designing all of the 36 building models, plastic hinges are defined and assigned for each member as illustrated in Chapter 2, then nonlinear static pushover analysis is done for these models using SAP2000 program. The pushover analysis for each model is stopped at a roof displacement where maximum base shear occurs since the definition of the yield and maximum roof displacements in this study were chosen according to (Park, 1988). In other words, the same approach used in Chapter 2 for the case study analysis is used for all of the 36 building models.

3.4 General Structural Behavior

As mentioned in Chapter 1, the presence of infill walls increases the lateral stiffness and strength of a building structure. In this study, it was found that most of the formation of the plastic hinges occurs in equivalent compression struts which represent the BCSM infill walls. Also, a high and sudden drop in the base shear has been noticed at roof displacement where maximum base shear occurs for all of the 36 building models. This is due to the high stiffness and strength of the equivalent compression struts that represent the BCSM infill walls. Figure B3.1 in Appendix B shows the performance of the elements for S11L7O60 model at roof displacement where maximum base shear occurs (equal 5783 kN) and Figure B3.2 in Appendix B shows the performance of the elements for the same building model without BCSM infill walls (S11L7O100 model) at roof displacement where maximum base shear occurs. As shown in Figure B3.1, most of the plastic hinges are formed at the equivalent compression struts whereas columns and beams still at the immediate occupancy range. However, for the same building model without BCSM infill walls as shown in Figure B3.2 in Appendix B, the plastic hinges are formed at columns and beams such that the plastic hinges of the bottom columns reached

the collapse prevention performance and the plastic hinges for the beams reached immediate occupancy, life safety and collapse prevention performance. Also, a sway due to gravity loads was noticed for all of the 36 building models.

Figure B3.3 in Appendix B shows the performance of the elements for S5L7O60 model at roof displacement where maximum base shear occurs (equal 7194 kN) and Figure B3.4 in Appendix B shows the performance of the elements for the same building model without BCSM infill walls (S11L7O100 model) at roof displacement where maximum base shear occurs.

3.5 Generating the Pushover Curves

Pushover curves are nessessary to estimate the C_d-Factors. The pushover curves for all of the 36 building models are showen in the following figures:

Figure 3.1

Pushover curves (Part one)

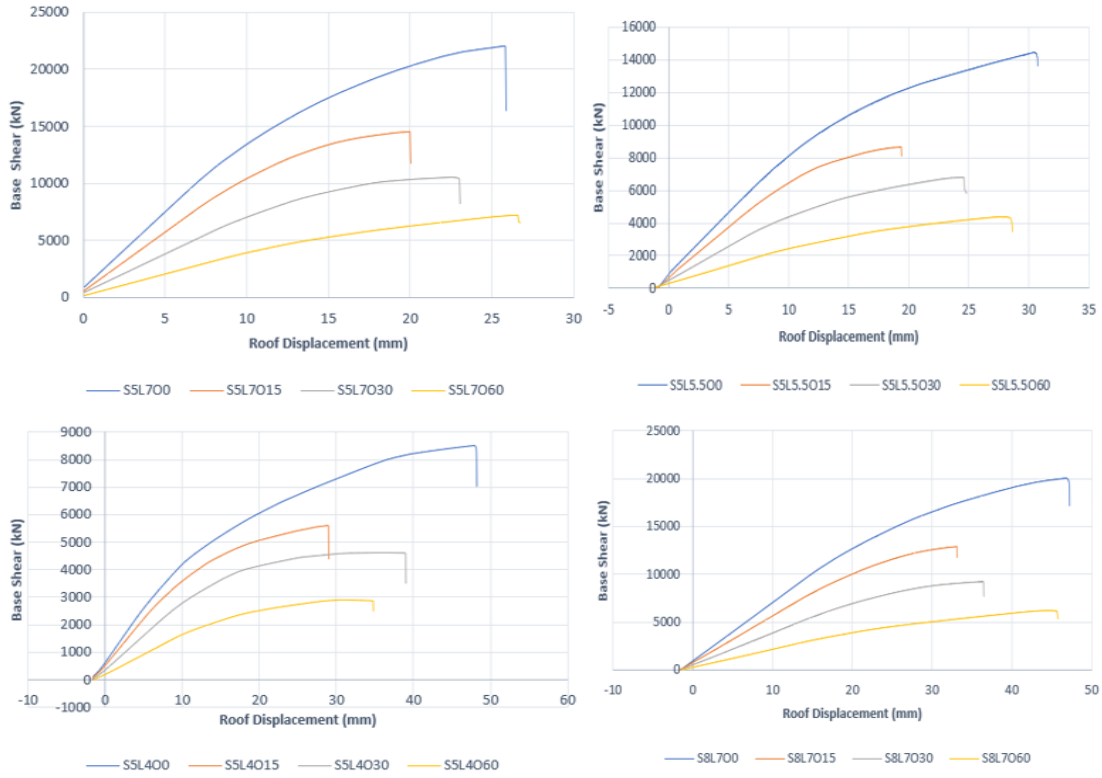

Figure 3.2

Pushover curves (Part two)

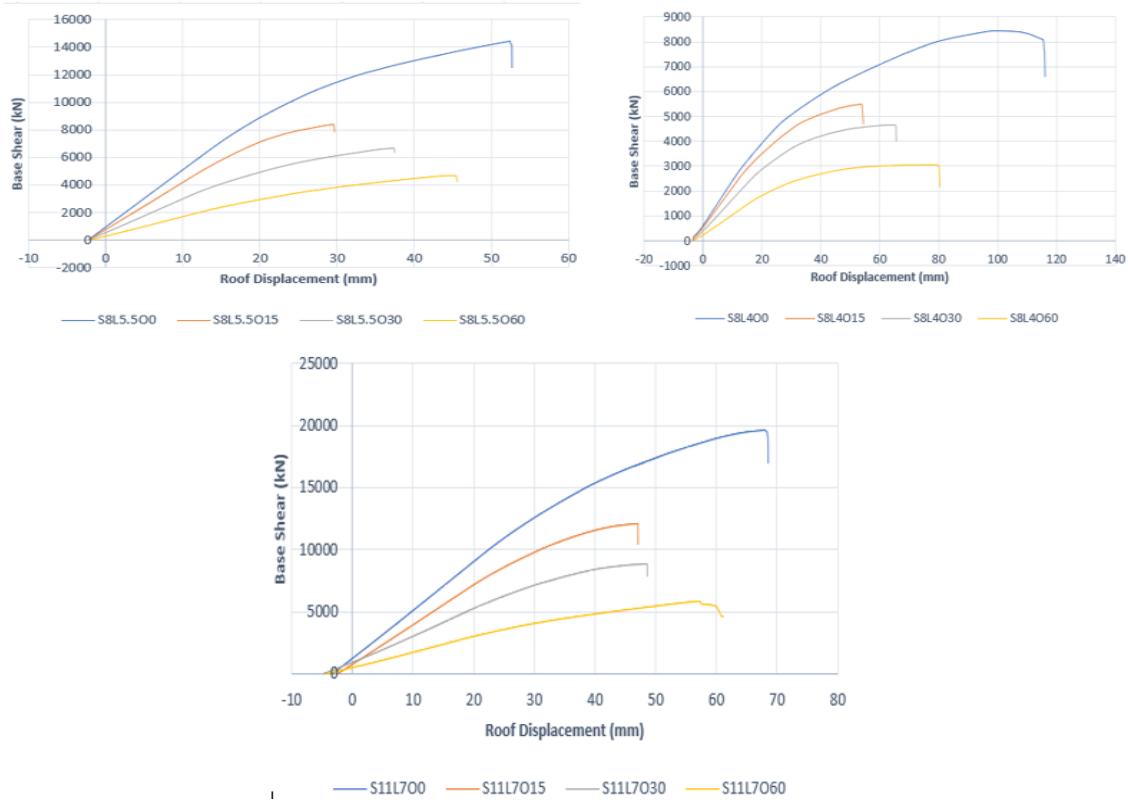

Figure 3.3

Pushover curves (Part three)

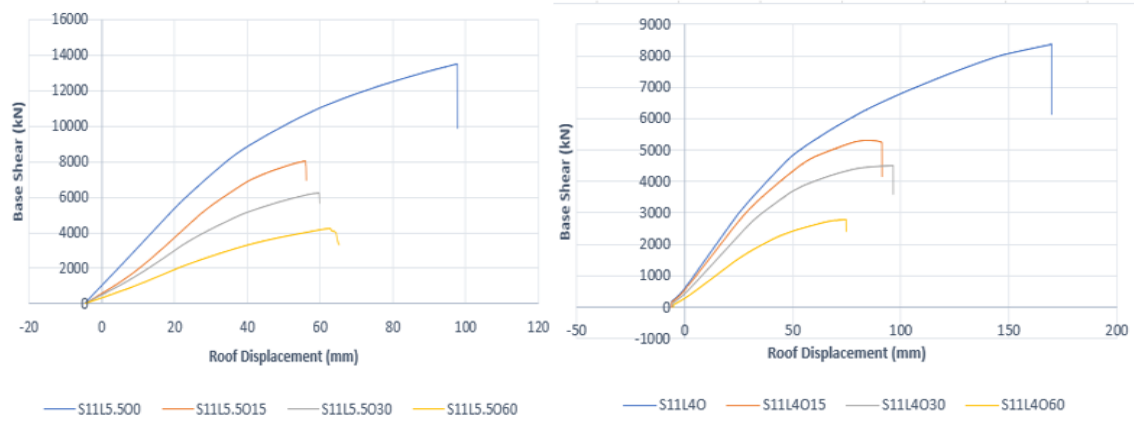

Also, Figure B3.5 in Appendix B shows the pushover curves for the same building models without BCSM infill walls (bare building models).

3.6 C_d-Factors Calculation

After computing the yield roof displacement, the maximum roof displacement, the yield base shear, and the design base shear for each building model according to what was mentioned in Section 1.7.6, the C_d-Factors are calculated as listed in Table 3.1.

Table 3.1

C_d-Factors for the building models

Model	Ro	μ	C_d (ΩXμ)	Model	Ro	μ	C_d (ΩXμ)
S5L7O0	10.78	1.41	15.20	S8L5.5O30	6.39	1.37	8.75
S5L7O15	7.92	1.42	11.25	S8L5.5O60	5.93	1.29	7.65
S5L7O30	7.02	1.45	10.18	S8L4O0	11.88	1.6	19.01
S5L7O60	6.31	1.28	8.08	S8L4O15	8.45	1.55	13.10
S5L5.5O0	10.16	1.46	14.83	S8L4O30	8.31	1.55	12.88
S5L5.5O15	6.84	1.44	9.85	S8L4O60	6.95	1.97	13.69
S5L5.5O30	6.57	1.44	9.46	S11L7O0	9.81	1.36	13.34
S5L5.5O60	5.87	1.33	7.81	S11L7O15	6.64	1.31	8.70
S5L4O0	11	1.61	17.71	S11L7O30	5.02	1.34	6.73
S5L4O15	8.02	1.65	13.23	S11L7O60	3.29	1.27	4.18
S5L4O30	7.84	1.91	14.97	S11L5.5O0	11.64	1.43	16.65
S5L4O60	6.61	1.53	10.11	S11L5.5O15	7.89	1.34	10.57
S8L7O0	10.02	1.37	13.73	S11L5.5O30	7.18	1.36	9.76
S8L7O15	7.58	1.31	9.93	S11L5.5O60	5.13	1.29	6.62
S8L7O30	6.03	1.37	8.26	S11L4O0	12.18	1.52	18.51
S8L7O60	4.84	1.28	6.20	S11L4O15	8.91	1.42	12.65
S8L5.5O0	10.58	1.46	15.45	S11L4O30	7.81	1.42	11.09
S8L5.5O15	6.71	1.33	8.92	S11L4O60	4.9	1.44	7.06

As shown in Table 3.2, there are a high value for the C_d-Factors compared to what is suggested by the ASCE7-16 code. This is mainly due to the high values of the overstrength factor for each building model since the lateral stiffness and strength that the BCSM infill walls add to a structure is very high. Also, Table 3.2 shows the C_d-factor for the bare building models with an average value of 5.1 which means that the ASCE7-16 code is unconservative in estimating the C_d factor for RC intermediate moment resisting frames. The coming section will illustrate the effect of the selected parameters in this study on the C_d-Factor.

Table 3.2

C_d-Factors for the bare building models

Model	*Ro*	μ	C_d
S5L4O100	2.32	1.3	3.03
S5L5.5O100	4	1.39	5.56
S5L7O100	4.09	1.35	5.53
S8L4O100	3.33	1.32	4.41
S8L5.5O100	3.97	1.28	5.09
S8L7O100	4.19	1.37	5.75
S11L4O100	3.99	1.61	6.4
S11L5.5O100	4.46	1.41	6.3
S11L7O100	3.02	1.19	3.59

3.7 Effect of The Parametric Study on the C_d-Factor

As mentioned in Section 3.2, the selected parameters in this study to find the effect of BCSM infill walls on the C_d-Factors for RC intermediate moment resisting frames are: the length of the BCSM infill wall, the opening ratio in the BCSM infill wall, and the number of stories of the building. The following subsections shows the effect of these parameters on the C_d-Factor.

3.7.1 Effect of BCSM Infill Walls Opening Ratio

The effect of the ratio of opening area to the BCSM infill wall area on the C_d-factor for the building models was studied. The results show that the increase of the BCSM infill walls opening ratio leads to a decrease in the C_d-Factor. This is mainly due to the reduction of the overstrength factor as the BCSM infill wall opening ratio increases. For example, a building model with 8 stories, with frames span length of 7 m, and with a %15 BCSM infill walls opening ratio decreased the C_d-Factor by %28 compared to the same building model with full walls (BCSM infill walls with %0 opening ration). When the opening ratio became %30, the C_d-Factor decreased by %40 compared to the same building model with full walls. Finally, When the opening ratio increased to %60, the C_d-Factor decreased by %54 compared to the same building model with full walls. Figure B3.6 in Appendix B shows an example for the variation of the overstrength factor for building models with 5 stories, 8 stories, and 11 stories and with frames span length of 5.5 m under the variation of the opening ratio of the BCSM infill wall.

3.7.2 Effect of BCSM Infill Walls Length

The effect of the BCSM infill walls length on the C_d-factor for the building models was studied. The results show that the increase of the BCSM infill walls length leads to a decrease in the C_d-Factor. Although the increase in a BCSM infill walls length leads to an increase of the lateral stiffness and strength for a one-bay RC frame, but this situation is different for the building models. This due to the increase in the aspect ratio of a building when the frames span length for it decrease. Lower aspect ratio of a building leads to higher ductility and a different lateral force distribution on the elements of the building model which leads to different values of the overstrength factor. For example, a building model with 11 stories, with a %0 BCSM infill walls opening ratio, and with frames span length of 4 m increased the C_d-Factor by %39 compared to the same building model with frames span length of 7 m. Also, when frames span length became 5.5 m the C_d-Factor increased by %11 compared to the same building model with frames span length of 7 m.

3.7.3 Effect of The Number of Stories of the Building

The number of stories of a building affect the fundamental period and the lateral force distribution of that building. Therefore, the effect of the number of stories of a building on the C_d-factor for the building models was studied. The results show that the C_d-Factor is not totally fixed to the number of stories of a building. In other words, it is not true that the increase in the number of stories will always leads to an increase in the C_d-Factor and vice versa. This is due to the compound effect between the overstrength and aspect ratio effect, thus ductility and lateral force distribution. For example, a building model with a %60 BCSM infill walls opening ratio, with frames span length of 4 m, and with 11 stories decreased the C_d-Factor by %31 compared to the same building model with 5 stories. But, a building model with a %60 BCSM infill walls opening ratio, with frames span length of 4 m, and with 8 stories increased the C_d-Factor by %35 compared to the same building model with 5 stories.

3.8 Proposed Formula to Estimate the C_d-Factor

One of the objectives of this study is to provide a simple formula that compute the C_d-Factor for buildings that have Perimeter BCSM infill walls. This is done using multivariate-linear regression using Excel program. According to the results in Table 3.2,

equation (3.1) shows the proposed formula for the C_d-Factor. The formula is for a factor Ψ that represents a percentage of the C_d-Factor suggested by the ASCE7-16 code for intermediate moment resisting frames. Table A3.2 in Appendix A shows the summary output for the multivariate-linear regression used to generate the formula for the Ψ factor.

$$\Psi = 0.55S + 0.6L - 0.1(S\ x\ L) - 2.6O \quad (3.1)$$

Where:

S: it is the number of stories in a building.
L: it is the BCSM infill walls length in a building (m).
O: it is the percentage of opening in the BCSM infill walls (the opening ratio).
For example, for S5L7O60 model:

Ψ= 0.55 x 5 + 0.6 x 7 – 0.1(5*7) – 2.6x0.6 = 1.89, so C_d = 1.89 x 4.5 = 8.5

The previous equation (equation (3.1)) assumes that the BCSM infill walls are included in the design process, meaning that their effect in adding stiffness and strength to the building is taken into consideration, but this does not really happen in the common design practice in Palestine. The common design practice only takes the effect of infill walls in terms of weight and mass and neglects the effect of infill walls in adding stiffness and strength to the building. Therefore, an analogy in this section will be used to generate a formula to estimate the C_d-Factor for buildings designed according to the common design practice.

If there are two adjacent structures, Section 12.12.3 in the ASCE7-16 code requires that they shall be structurally separated by a distance sufficient to avoid damaging contact. To do so, ASCE7-16 code suggested an equation (equation 12.12-1 in the ASCE7-16) to find that separation distance. Usually, this equation results a high value which leads to a difficulty in implementation for construction workers and leads to additional costs.

To take advantage of the presence of BCSM infill walls, a formula to estimate the C_d-Factor for buildings designed according to the common practice is suggested in this study. According to equation (1.14), the C_d-Factor can be calculated by dividing Δmax by Δd. According to the common practice, Δd is estimated without taking the effect of infill walls in adding stiffness and strength to the building. Therefore, Δd for each building

model is found without taking the effect of infill walls in adding stiffness and strength, but taking the effect of BCSM infill walls on the fundamental period of the building model thus the base shear, then Δmax is divided by Δd to find the C_{ds}-Factor for each building model where C_{ds} represents the deflection amplification factor for buildings designed according to the common design Practice in Palestine. After that, a formula for the factor Ψ_S that represents a percentage of the C_d-Factor suggested by the ASCE7-16 code for intermediate moment resisting frames is generated. Table 3.3 shows the results of the C_{ds}-Factor that take in consider the common design practice in Palestine. In other words, the formula is to guide structural engineers in Palestine to find the inelastic displacement of buildings that have BCSM infill walls by multiplying the inaccurate elastic displacement that they find for bare building models (since the common design practice in Palestine neglect the effect of BCSM infill walls on the drift and strength of the building) with the Ψ_S -Factor and the C_d-Factor for IMRF (4.5) to estimate an accurate inelastic displacement for the buildings.

Table 3.3

The results of the C_{ds}-Factor that take in consider the common design practice in Palestine

Model	$\Delta \max(mm)$	$\Delta d(mm)$	C_{ds}	Model	$\Delta\max(mm)$	$\Delta d(mm)$	C_{ds}
S5L7O0	25.75	12.97	1.99	S8L5.5O30	38.34	18.6	2.77
S5L7O15	19.9	13	2.18	S8L5.5O60	44.73	14.6	3.06
S5L7O30	22.58	9.64	2.34	S8L4O0	99.27	27.5	3.61
S5L7O60	26.48	8.12	3.26	S8L4O15	53.7	25.6	3.44
S5L5.5O0	30.55	14.37	2.13	S8L4O30	65.19	22.7	4.28
S5L5.5O15	19.44	12.65	1.54	S8L4O60	79	18.2	4.34
S5L5.5O30	24.63	10.83	2.27	S11L7O0	68	34.4	1.98
S5L5.5O60	27.73	9.96	2.78	S11L7O15	46.94	22.2	2.11
S5L4O0	47.97	19.31	2.48	S11L7O30	48.47	30.8	2.25
S5L4O15	29.8	16.4	2.26	S11L7O60	57.29	31.5	2.25
S5L4O30	36.2	14.25	2.54	S11L5.5O0	97.53	31.2	3.13
S5L4O60	30.68	11.55	2.66	S11L5.5O15	50.9	29	2.74
S8L7O0	46.9	24.1	1.95	S11L5.5O30	55.53	25.6	3.36
S8L7O15	33.07	21.7	2.04	S11L5.5O60	59.55	25.2	4.04
S8L7O30	36.37	18.2	2.00	S11L4O0	169.9	66.6	2.55
S8L7O60	44.4	15.4	2.88	S11L4O15	83.34	35.47	2.17
S8L5.5O0	52.48	23.2	2.26	S11L4O30	82.7	35.4	2.84
S8L5.5O15	31.2	21.8	2.36	S11L4O60	74.42	35.9	2.95

From the results of Table 3.4, a formula to estimate the Ψ_S factor is generated using multivariate-linear regression. Equation (3.2) shows the proposed formula for the factor

Ψ_S. Table A3.3 in Appendix A shows the summary output for the multivariate-linear regression used to generate the formula for the Ψ_S factor that take in consider the common design practice in Palestine and Figure B3.7 in Appendix B shows the residuals for each term in the Ψ_S factor formula.

$$\Psi s = 0.08S + 0.084L - 0.015(SxL) + 0.22O \quad (3.2)$$

Where:

S: it is the number of stories in a building.
L: it is the BCSM infill walls length in a building (m).
O: it is the percentage of opening in the BCSM infill walls (the opening ratio).

The previous formula (equation (3.2)) is valid for: buildings whose number of stories ranges from 5 to 11 stories, whose frames span length (center to center) ranges from 4m to 7m, and for building that include perimeter BCSM infill walls with an opening ratio ranges from %0 to %60. Also, the effect of BCSM infill walls on the fundamental period of the building thus the base shear shall be taken into consideration to use that formula.

Verification of equation (3.2) is done in this study to verify the validity of that equation. This is done by modeling a different 6 building models under different scenarios of parameters. The width of the equivalent compression strut for each of the 6 building models is found using equation (1.13). The plastic hinge properties for each of the 6 building models is found using linear interpolation from the result in Table 2.2 as shown in Table 3.4. For example, for S5L4.5O30 model, the force-deformation parameters (F1, F2, U1, U2, …etc) is found by linear interpolating these force-deformation parameters from models S5L4O30 and S5L5.5O30. Table 3.5 shows the verification results of equation (3.2), and Figure B3.8 shows the pushover curves for the 6 building models.

Table 3.4

Plastic hinge properties for the 6 building models

BCSM Infill Wall Length	BCSM Infill Wall Opening Ratio	F1 (kN)	F2 (kN)	F3 (kN)	F4 (kN)	U1 (mm)	U2 (mm)	U3 (mm)	U4 (mm)
4.5	0.3	606	827.5	864.7	945.8	1.61	2.41	5.77	8.97
6	0.15	1106.3	1500.16	1575.4	1398.8	1.5	2.15	3.99	5.75
4.5	0	1470	2044.4	2173	2044.2	1.65	2.58	5.39	8.07
5	0.3	613	857.1	931	911.2	1.63	2.53	5.46	7.96
6.5	0.15	1220.67	1651.21	1742.25	1607.2	1.51	2.31	3.87	5.61
6	0.6	373.33	513.33	594.06	553	2.09	3.02	6.02	6.81

Table 3.5

The verification results of equation (3.2)

Model	$\Delta max\ (mm)$	$\Delta d\ (mm)$	C_d	C_{ds}=$\Psi X 4.5$	Difference (%)
S5L4.5O30	39.4	18.1	2.18	2.27	4.1
S7L6O15	28.9	13.76	2.1	2.4	14.28
S10L4.5O0	96.6	39.1	2.47	2.26	8.5
S7L5O30	41.5	17.4	2.38	2.76	16
S5L6.5O15	22	11.6	1.9	2.21	16.3
S9L6O60	51	15.1	3.38	3.1	8.3

Chapter Four
Conclusions, Recommendations, and Future Work

4.1 Summary

This thesis explored the variation of the deflection amplification factor of intermediate moment resisting frames under the presence of perimeter BCSM infill walls. It has been noticed that BCSM infill walls results a high value of the C_d-Factor due to their effect in adding lateral stiffness and strength to the structure.

To study the effect of perimeter BCSM infill walls on the deflection amplification factor for intermediate moment resisting frames, a 36 building models were selected and simulated using the finite element program SAP2000.

The 36 building models were designed and analyzed for several scenarios of parameters. The parameters are: the length of the BCSM infill wall, the opening ratio in the BCSM infill wall, and the number of stories of the building. Nonlinear static pushover analysis was performed to generate load-deflection curves for the several scenarios of parameters. These curves were used to estimate the C_d-factor under the variation of the parameters.

After getting the results, two formulas were proposed to estimate the C_d-Factor. The first formula is to estimate the C_d-Factor if BCSM infill walls is considered in the design process in terms of its effect on the lateral stiffness and strength to the structure. Since the common design practice in Palestine only takes the effect of BCSM infill walls in terms of weight and mass, a second formula to estimate the C_d-Factor were proposed to help engineers in Palestine to get benefit of having BCSM infill walls.

4.2 Conclusions

According to the results of this thesis, the main conclusions are:

1. The C_d-Factor is very sensitive to the presence of BCSM infill walls; it can lead to a significant change in the C_d-Factor which may reach 4.2 times compared to what is suggested by the ASCE7-16 code.
2. The increase of the BCSM infill walls opening ratio leads to a decrease in the C_d-Factor.
3. The increase of the BCSM infill walls length leads to a decrease in the C_d-Factor.

4. The C_d-Factor is not totally fixed to the number of stories of a building. In other words, it is not true that the increase in the number of stories will always leads to an increase in the C_d-Factor and vice versa.
5. Results were used to develop simple two formulas to estimate the C_d-Factor; one is general and the other is to help engineers in Palestine to get benefit of having BCSM infill walls.

4.3 Limitation of this Study

In this study, the results are confined by assumptions made within the scope of this study. These limitations are:

1. Structural irregularities were not taken into account in this study and the analysis was done for regular buildings.
2. The impacts of soil-structure interactions were not taken into account in this study.
3. The equivalent compression struts were assumed to act at the center of the columns where the effect of eccentricity is neglected.
4. The two-proposed formulas are valid for: buildings whose number of stories ranges from 5 to 11 stories, whose frames span length (center to center) ranges from 4m to 7m, and for building that include perimeter BCSM infill walls with an opening ratio ranges from %0 to %60.

4.4 Recommendations and Future Work

To extend the scope of this study, certain aspects could be further explored within this research. These aspects may include:

1. Repeating the same analysis using nonlinear time-history analysis.
2. Studying the effect of BCSM infill walls on the structural irregularities such as the soft-story irregularity.
3. Studying the effect of BCSM infill walls on the structural irregularities such as the soft-story irregularity.
4. Studying the effect of BCSM infill walls on the response modification factor.
5. Introduce the effect of soil-structure interactions as a substructure in the building.

List of Abbreviations

Abbreviation	Meaning
$\mathbf{S_{DS}}$	The design, 5% damped, spectral response acceleration parameter at short periods as defined in Section 11.4.5 in the ASCE7-16 code
$\frac{\boldsymbol{Kpc}}{\boldsymbol{Ke}}$	Ratio between the post-capping stiffness (Kpc) and the initial stiffness (Ke)
$\frac{\boldsymbol{dc}}{\boldsymbol{ld}}$	Axial deformation of the infill strut at peak strength (dc) normalized by the length of the strut (ld)
$\boldsymbol{S_{D1}}$	The design, 5% damped, spectral response acceleration parameter at a period of 1 s as defined in Section 11.4.5 in the ASCE7-16 code
$\mathbf{\Delta d}$	Displacement at the design base shear
Δmax	Maximum displacement corresponding to the peak base shear of the pushover curve
$\boldsymbol{\Delta y}$	Yield displacement, calculated by reduced stiffness method
C_d	Deflection amplification factor
C_{ds}	Deflection amplification factor for the common design Practice in Palestine
$\boldsymbol{Cs}$	Seismic response coefficient
d_{inf}	Length of the diagonal strut
Dmax	Maximum nonlinear displacement during an earthquake
Ds	Elastic displacement during an earthquake
$\boldsymbol{Em}$	Masonry modulus of elasticity
$\boldsymbol{f'c}$	Compressive strength of concrete
Fc	Capping strength
$F_{Collapse}$	Collapse load
fm,	Compressive strength of the infill
Fres	Residual strength
Fy	Yield strength
$\boldsymbol{hn}$	Height of the structure
$\boldsymbol{Ie}$	Importance factor
$\boldsymbol{k}$	Lateral stiffness of the structure
$\boldsymbol{Ke}$	Initial stiffness
$\boldsymbol{kW}$	Express the prevailing failure mode
$\boldsymbol{L}$	BCSM infill walls length in a building
$\boldsymbol{lw}$	Length of the infill panel
$\boldsymbol{m}$	Mass of the structure
Mub	Ultimate moment for the beam
Muc	Ultimate moment for the column
Myb	Yielding moment for the beam
Myc	Yielding moment for the column
$\boldsymbol{N}$	Number of stories above the base
$\boldsymbol{O}$	Percentage of opening in the BCSM infill walls
Øyc	Curvature of the column at yield
$\boldsymbol{q}$	Deflection amplification factor according to the Euro code
$\boldsymbol{q0}$	Main value for the response factor
R	Response modification factor
RC	Reinforced concrete
$\boldsymbol{Ro}$	Overstrength factor
$\boldsymbol{S}$	Number of stories in a building
$\boldsymbol{t}$	Thickness of the plain concrete wall
$\boldsymbol{T}$	The fundamental period of the structure
$\boldsymbol{Ta}$	Approximate fundamental period

$\boldsymbol{tw}$	Thickness of the infill panel
$\boldsymbol{Vd}$	Design base shear
$\boldsymbol{Vy}$	Ideal yield base shear
$\boldsymbol{W}$	Width of the diagonal strut
$\boldsymbol{W}$	Effective seismic weight
$\boldsymbol{Wa}$	Equivalent strut width of the stone wall
$\boldsymbol{\mu s}$	Ductility factor
$\boldsymbol{\lambda h}$	Length of the horizontal contact between the diagonal strut and frame
Ψ	Factor represents a percentage of the Cd-Factor suggested by the ASCE7-16 code for intermediate moment resisting frames
Ψ_s	Factor represents a percentage of the Cd-Factor suggested by the ASCE7-16 code for intermediate moment resisting frames for the common design practice in Palestine

References

Abdel-Halim, M. A. H., & Barakat, S. A. (2003). Cyclic performance of concrete-backed stone masonry walls. *Journal of Structural Engineering*, *129*(5), 596–605.

Abdelkareem, K. H., Abdel Sayed, F. K., Ahmed, M. H., & Al-Mekhlafy, N. (2013). Equivalent strut width for modeling RC infilled frames. *JES. Journal of Engineering Sciences*, *41*(3), 851–866.

AbdelRahman, B., & Galal, K. (2022). Sensitivity of the seismic response of reinforced concrete masonry walls with boundary elements to design parameters. *Engineering Structures*, *255*, 113953.

Akhoundi, F., Lourenço, P. B., & Vasconcelos, G. (2016). Numerically based proposals for the stiffness and strength of masonry infills with openings in reinforced concrete frames. *Earthquake Engineering & Structural Dynamics*, *45*(6), 869–891.

Albayrak, U., Ünlüoğl, E., & Doğan, M. (2017). An overview of the modelling of infill walls in framed structures. *International Journal of Structural and Civil Engineering Research*, *6*(1), 24–29.

Al-Dabbeek, J. N., & El-Kelani, R. J. (2008). Rapid assessment of seismic vulnerability in Palestinian refugee camps. *Journal of Applied Sciences*, *8*(8), 1371–1382.

Alguhane, T. M., Khalil, A. H., Fayed, M. N., & Ismail, A. M. (2016). Modeling of masonry in-filled R/C frame to evaluate seismic performance of existing building. *International Journal of Civil and Environmental Engineering*, *9*(10), 1387–1398.

Al-Hroub, A. (2022). *Investigation the Behavior of RC Frame With Stone Infill Wall Using Micro Modeling Approach*. An-Najah National University.

Al-Nimry, H. S. (2014). Quasi-static testing of RC infilled frames and confined stone-concrete bearing walls. *Journal of Earthquake Engineering*, *18*(1), 1–23.

Aninthaneni, P. K., & Dhakal, R. P. (2016). Prediction of fundamental period of regular frame buildings. *Bulletin of the New Zealand Society for Earthquake Engineering*, *49*(2), 175–189.

Asteris, P. G., Tsaris, A. K., Cavaleri, L., Repapis, C. C., Papalou, A., Di Trapani, F., & Karypidis, D. F. (2016). Prediction of the fundamental period of infilled RC frame structures using artificial neural networks. *Computational Intelligence and Neuroscience*, *2016*(1), 5104907.

Cavaleri, L., Fossetti, M., & Papia, M. (2004). Effect of vertical loads on lateral response of infilled frames. *Proceedings 13th World Conference on Earthquake Engineering*.

Chopra, A. K. (1995). *Dynamics of Structures Dynamics of Structures - Theory and Applications to Earthquake Engineering*. Prentice Hall.

Chopra, A. K., & Goel, R. K. (2000). Building period formulas for estimating seismic displacements. *Earthquake Spectra*, *16*(2), 533–536.

Chrysostomou, C. Z. (1991). *Effects of degrading infill walls on the nonlinear seismic response of two-dimensional steel frames*. Cornell University.

Dautaj, A. D., Kadiri, Q., & Kabashi, N. (2018). Experimental study on the contribution of masonry infill in the behavior of RC frame under seismic loading. *Engineering Structures*, *165*, 27–37.

De Angelis, A., & Pecce, M. R. (2019). The structural identification of the infill walls contribution in the dynamic response of framed buildings. *Structural Control and Health Monitoring*, *26*(9), e2405.

Eleftheriadou, A. K., Karabinis, A. I., & Baltzopoulou, A. D. (2012). Fundamental period versus seismic damage for reinforced concrete buildings. *Proc. 15th World Conf. Earthq. Eng. Lisboa*.

Furtado, A., Rodrigues, H., Arêde, A., & Varum, H. (2016). Simplified macro-model for infill masonry walls considering the out-of-plane behaviour. *Earthquake Engineering & Structural Dynamics*, *45*(4), 507–524.

Gaetani d'Aragona, M., Polese, M., & Prota, A. (2021). *Effect of Masonry Infill Constitutive Law on the Global Response of Infilled RC Buildings. Buildings; 11 (2), 57*.

Halahla, M. (2019). *Influence of Bearing Non-Reinforced Parameter Walls with Stone Cladding on Fundamental Period Computation*. An-Najah National University.

Huang, H., Burton, H. V, & Sattar, S. (2020). Development and utilization of a database of infilled frame experiments for numerical modeling. *Journal of Structural Engineering*, *146*(6), 04020079.

Jinya, M. H., & Patel, V. R. (2014). Analysis of RC frame with and without masonry infill wall with different stiffness with outer central opening. *International Journal of Research in Engineering and Technology*, *3*(6), 76–83.

Kose, M. M. (2009). Parameters affecting the fundamental period of RC buildings with infill walls. *Engineering Structures*, *31*(1), 93–102.

Li, S., Kose, M. M., Shan, S., & Sezen, H. (2019). Modeling methods for collapse analysis of reinforced concrete frames with infill walls. *Journal of Structural Engineering*, *145*(4), 04019011.

Mainstone, R. J. (1971). On the stiffness and strength of infilled frames. *Proc Inst Civil Eng*, *49*, 57.

Mainstone, R. J., & Weeks, G. A. (1972). *The influence of a bounding frame on the racking stiffness and strengths of brick walls*. Building Research Station.

Manju, G. (2014). Dynamic Analysis of Infills on RC Framed Structures. *International Journal of Innovative Research in Science, Engineering and Technology*, *3*(9), 16150–16158.

Mondal, G., & Jain, S. K. (2008). Lateral stiffness of masonry infilled reinforced concrete (RC) frames with central opening. *Earthquake Spectra*, *24*(3), 701–723.

Öztürkoğlu, O., & Ucar, T. (2019). Influence of Opening Ratio and Position in Infill Wall on Constitutive Law of Equivalent Compression Strut. *European Journal of Engineering and Natural Sciences*, *3*(2), 57–64.

Ozturkoglu, O., Ucar, T., & Yesilce, Y. (2017). Effect of masonry infill walls with openings on nonlinear response of reinforced concrete frames. *Earthquakes and Structures*, *12*(3), 333–347.

Park, R. (1988). Ductility evaluation from laboratory and analytical testing. *Proceedings of the 9th World Conference on Earthquake Engineering*, *8*, 605–616.

Paulay, T., & Priestley, M. J. N. (1992). *Seismic design of reinforced concrete and masonry buildings* (Vol. 768). Wiley New York.

Polyakov, S. V. (1960). On the interaction between masonry filler walls and enclosing frame when loaded in the plane of the wall. *Translations in Earthquake Engineering*, *2*(3), 36–42.

Qarout, O. (2018). *The Effect of Various Patterns of Internal Partitions on the Fundamental Period of Reinforced Concrete Framed Buildings Experimental and FE Modelling Study*. An-Najah National University.

Samimifar, M., Oskouei, A. V., & Rofooei, F. R. (2015). Deflection amplification factor for estimating seismic lateral deformations of RC frames. *Earthquake Engineering and Engineering Vibration*, *14*, 373–384.

Sattar, S., & Liel, A. B. (2010). Seismic performance of reinforced concrete frame structures with and without masonry infill walls. *9th US National and 10th Canadian Conference on Earthquake Engineering*.

Shendkar, M. R., Kontoni, D.-P. N., Işık, E., Mandal, S., Maiti, P. R., & Harirchian, E. (2022). Influence of Masonry Infill on Seismic Design Factors of Reinforced-Concrete Buildings. *Shock and Vibration*, *2022*(1), 5521162.

Uang, C.-M. (1991). Establishing R (or R w) and C d factors for building seismic provisions. *Journal of Structural Engineering*, *117*(1), 19–28.

FEMA.2000.Prestandard and Commentary for the Seismic Rehabilitation of Buildings. Rehabilitation Requirements.

Uang, C. M., & Maarouf, A. (1994). Deflection amplification factor for seismic design provisions. Journal of structural engineering. 120(8), 2423-2436.

Code, P. (2004). Eurocode 8: Design of structures for earthquake resistance-part 1: general rules, seismic actions and rules for buildings. Brussels: EuropeanCommittee for Standardization.

American Society of Civil Engineers. 2010. Minimum Design Loads for Buildings and Other Structures, ASCE Standard,. ASCE standard.

UBC (1997) Uniform Building Code. International Conference of Building Officials. Whittier, California, USA

SAP2000 (2025) Integrated Software for Structural Analysis and Design: Computers and Structures. Inc.Berkeley, California.

ACI Committee 318. 2014. Aci 318-14 Building Code Requirements for Structural Concrete (ACI 318-14) and Commentary (ACI 318R-14).

Stafford Smith, B., & Carter, C. (1969). A method of analysis for infilled frames. Proceedings of the institution of civil engineers, 44(1), 31-48.

NEHRP, Recommended Provisions for Seismic Regulations for New Buildings, Building Seismic Safety Council, Washington, D.C, 2000.

Mander, J.B., M.J.N. Priestley, and R. Park 1984. Theoretical StressStrain Model for Confined Concrete. Journal of Structural Engineering.ASCE. 114(3). 1804-1826.

Appendices

Appendix A

Tables

Table A1.1

Table 12.8-2 in the ASCE7-16 code, for Ct and x parameters in metric units.

Structure type	C_t	x
Moment-resisting frame systems in which the frames resist 100% of the required seismic force and are not enclosed or adjoined by components that are more rigid and will prevent the frames from deflecting where subjected to seismic forces:		
Steel moment-resisting frames	0.0724	0.9
Concrete moment-resisting frames	0.0466	0.9
Steel eccentrically braced frames in accordance with Table 12.2-1 lines B1 or D1	0.0731	0.75
Steel buckling-restrained braced frames	0.0731	0.75
All other structural systems	0.0488	0.75

Table A1.2

Database sources that were assembled by Huang et al. (2020).

Reference	Number ofspecimens	Frame type	Loading type
Abdul-Kadir (1974)	12	Steel	Monotonic
Akhoundi et al. (2018)	1	RC	Quasi-static cyclic
Al-Chaar et al. (2002)	4	RC	Monotonic
Angel et al. (1994)	7	RC	Quasi-static cyclic
Anil and Altin (2007)	7	RC	Quasi-static cyclic
Baran and Sevil (2010)	3	RC	Quasi-static cyclic
Basha and Kaushik (2016)	9	RC	Quasi-static cyclic
Bergami and Nuti (2015)	2	RC	Quasi-static cyclic
Billington et al. (2009)	1	RC	Quasi-static cyclic
Blackard et al. (2009)	4	RC	Quasi-static cyclic
Bose and Rai (2014)	I	RC	Quasi-static cyclic
Calvi and Bolognini (2008)	4	RC	Quasi-static cyclic
Cavaleri and Di Trapani (2014)	12	RC	Quasi-static cyclic
Chiou and Hwang (2015)	4	RC	Quasi-static cyclic
Colangelo (2005)	11	RC	Pscudo-dynamic
Combescure ct al. (1996)	2	RC	Quasi-static cyclic
Crisafulli (1997)	2	RC	Quasi-static cyclic
Da Porto et al. (2013)	6	RC	Quasi-static cyclic
Dautaj et al. (2018)	7	RC	Quasi-static cyclic
Dawe and Scah (1989)	28	Steel	Monotonic
Fiorato et al. (1970)	7	RC	Monotonic
Flanagan and Bennett (1999)	8	Steel	Quasi-static cyclic
Gazic and Sigmund (2016)	11	RC	Quasi-static cyclic
Haider (1995)	4	RC	Quasi-static cyclic
Kakaletsis and Karayannis (2008)	6	RC	Quasi-static cyclic
Khoshnoud and Marsono (2016)	2	RC	Monotonic

Kumar et al. (2016)	1	RC	Quasi-static cyclic
Leuchars and Scrivener (1976)*	2	RC	Quasi-static cyclic
Liu and Soon (2012)	10	Steel	Monotonic
Mansouri et al. (2014)	5	RC	Quasi-static cyclic
Markulak et al. (2013)	6	Steel	Quasi-static cyclic
Mehrabi et al. (1996)	10	RC	Monotonic/ Quasi-static cyclic
Misir et al. (2016)	5	RC	Quasi-static cyclic
Morandi et al. (2014)	4	RC	Quasi-static cyclic
Mosalam et al. (1997)	4	Steel	Quasi-static cyclic
Pires et al. (1997)	2	RC	Quasi-static cyclic
Schwarz et al. (2015)	3	RC	Quasi-static cyclic
Sigmund and Penava (2013)	9	RC	Quasi-static cyclic
Stylianidis (2012)	5	RC	Quasi-static cyclic
Tasnimi and Mohebkhah (2011)	5	Steel	Quasi-static cyclic
Tawfik Essa et al. (2014)	3	RC	Quasi-static cyclic
Tizapa (2009)	3	RC	Quasi-static cyclic
Verderame et al. (2016)	2	RC	Quasi-static cyclic
Waly (2000)	2	RC	Quasi-static cyclic
Yorulmaz and Sozen (1968)	7	RC	Monotonic
Yuksel and Teymur (2011)	2	RC	Quasi-static cyclic
Zarnic and Tomazevic (1985)	3	RC	Quasi-static cyclic
Zhai et al. (2016)	3	RC	Quasi-static cyclie
Zovkic et al. (2013)	3	RC	Quasi-static cyclic

Table A1.3

Empirical formulas for the backbone curve parameters that represent the nonlinear axial response of the infill equivalent compression struts.

Parameter	Description	Unit	Empirical Formula
Ke	Initial stiffness	kN/mm	$K_e = 0.0143E_m^{0.618}t_w^{0.694}\left(\frac{h_w}{l_w}\right)^{-1.096}$
Fc	Capping strength	kN	$F_c = 0.003766f_m^{0.196}t_w^{0.867}l_d^{0.792}$
Fy	Yield strength	kN	$F_y = 0.72F_c$
Fres	Residual strength	kN	$F_{res} = 0.4F_c$
$\frac{dc}{ld}$	Axial deformation of the infill strut at peak strength (dc) normalized by the length of the strut (ld)		$\frac{d_c}{l_d} = 0.0154E_m^{-0.197}\left(\frac{h_w}{l_w}\right)^{0.978}$
$\frac{Kpc}{Ke}$	Ratio between the post-capping stiffness (Kpc) and the initial stiffness (Ke)		$\frac{K_{pc}}{K_e} = -1.278f_m^{-0.357}t_w^{-0.517}$

Where fm, Em, lw, tw are the compressive strength of the infill, the masonry modulus of elasticity, the length of the infill panel, and the thickness of the infill panel, respectively.

(Huang et al., 2020).

Table A1.4

C_d values for moment resisting frame system in the ASCE 7-16 code .

Moment Resisting Frame Systems	C_d
1. Steel special moment frames	5.5
2. Steel special truss moment frames	5.5
3. Steel intermediate moment frames	4
4. Steel ordinary moment frames	3
5. Special reinforced concrete moment frames	5.5
6. Intermediate reinforced concrete moment frames	4.5
7. Ordinary reinforced concrete moment frames	2.5
8. Steel and concrete composite special moment frames	5.5
9. Steel and concrete composite intermediate moment frames	4.5
10. Steel and concrete composite partially restrained moment frames	5.5
11. Steel and concrete composite ordinary moment frames	2.5
12. Cold-formed steel-special bolted moment frame	3.5

Table A1.5

Response Factor q0 values according to the Euro code.

Structural type		***q0***
Frame system		5.0
Dual system	Frame equivalent	5.0
	Wall equivalent, with coupled walls	5.0
	Wall equivalent, with uncoupled walls	4.5
Wall system	with coupled walls	5.0
	with uncoupled walls	4.0
Core system		3.5
Inverted pendulum system		2.0

Table A1.6

R Factor according to the Egyptian seismic code

Lateral force resisting system	Ductility	R
RC Moment resisting frame	Sufficient	7
	Not Sufficient	5

Table A2.1

The characteristic of the structural elements

Structural Element	Depth (cm)	Width (cm)	Longitudinal Reinforcement	Ties
Columns	50	50	12Ø18	4Ø10 mm/m
Beams	50	50	Top reinforcement.: 8Ø18 Bottom reinforcement: 5Ø16	2Ø10 mm/ 12cm
Struts	16.26	76.4	----------	----------

4 cm cover for beams and columns reinforcement.

Table A2.2

The properties of the materials used

Element	Concrete Compressive Strength (MPa)	Modulus of Elasticity of Concrete (MPa)	Min. Yield Strength of A615 Grade 60 Steel (MPa)	Modulus of Elasticity of A615 Grade 60 Steel (GPa)
Columns	28	24870	414	200
Beams	24	23025	414	200
Struts	16.6	191491	----------	----------

Table A2.3

Weight of BCSM infill wall calculations for one-meter length and 3.12-meter height

Component	Width (m)	Unit Weight (kN/m3)	One meter length x 3.12 meter height Weight (kN)
Stone layer	0.04	27	3.3696
Plain concrete	0.12	22	9.36
Brick	0.1	12	3.744
Sum			16.4736

Table A2.4

Summary of the adopted vertical loads

Load Type	Design Load	Magnitude	Unit
Dead Load	Own-weight of the slab	5	kN/m^2
	Superimposed Dead Load	4	kN/m^2
		16.5 for perimeter beams	kN/m
Live Load	Residential Building	3	kN/m^2

Table A2.5

Soil classification

Site Class	vs	N or Nch	su
A. Hard rock	>5,000 ft/s	NA	NA
B. Rock	2,500 to 5,000 ft/s	NA	NA
C. Very dense soil and soft rock	1,200 to 2,500 ft/s	>50 blows/ft	>2,000 lb/ft^2
D. Stiff soil	600 to 1,200 ft/s	15 to 50 blows/ft	1,000 to 2,000 lb/ft2
E. Soft clay soil	<600 ft/s	<15 blows/ft	< 1,000 lb/f^2
F. Soils requiring site response analysis in accordance with Section 2.1	see Section 20.3.1		

(ASCE7-16,2016).

Table A2.6

Normalization of the fundamental mode shape vector.

Story Number	Normalized in X-direction
5	1
4	0.888
3	0.711
2	0.484
1	0.224

Table A2.7

The reinforcement detailing and the geometrical properties of the RC frame.

Element	Depth (cm)	Width (cm)	Reinforcement
Columns	70	25	4Ø25
Beam	40	25	3Ø14 bot. rein. 2Ø14 top rein.

Table A3.1

The properties of the 36 building models.

Model	BCSM Infill Wall Length (m)	BCSM Infill Wall Opening Ratio (%)	Number of Stories of the Model
S5L7O0	7	0	5
S5L7O15	7	15	5
S5L7O30	7	30	5
S5L7O60	7	60	5
S5L5.5O0	5.5	0	5
S5L5.5O15	5.5	15	5
S5L5.5O30	5.5	30	5
S5L5.5O60	5.5	60	5
S5L4O0	4	0	5
S5L4O15	4	15	5
S5L4O30	4	30	5
S5L4O60	4	60	5
S8L7O0	7	0	8
S8L7O15	7	15	8
S8L7O30	7	30	8
S8L7O60	7	60	8
S8L5.5O0	5.5	0	8
S8L5.5O15	5.5	15	8
S8L5.5O30	5.5	30	8
S8L5.5O60	5.5	60	8
S8L4O0	4	0	8
S8L4O15	4	15	8
S8L4O30	4	30	8
S8L4O60	4	60	8
S11L7O0	7	0	11
S11L7O15	7	15	11
S11L7O30	7	30	11
S11L7O60	7	60	11
S11L5.5O0	5.5	0	11
S11L5.5O15	5.5	15	11
S11L5.5O30	5.5	30	11
S11L5.5O60	5.5	60	11
S11L4O0	4	0	11
S11L4O15	4	15	11
S11L4O30	4	30	11
S11L4O60	4	60	11

Where:

S8L7O15: The name of the model mentions a building model with 8 stories, frames span length of 7m (same as BCSM infill walls length), and a BCSM infill walls with opening ratio of %15.

Table A3.2

The summary output for the multivariate-linear regression used to generate the formula for the Ψ factor

SUMMARY OUTPUT								
Regression Statistics								
Multiple R	0.982705219							
R Square	0.965709548							
Adjusted R Square	0.931244818							
Standard Error	0.517579283							
Observations	36							
ANOVA								
	df	*SS*	*MS*	*F*	*Significance F*			
Regression	4	241.4221229	60.35553073	225.3010956	1.96058E-22			
Residual	32	8.572426062	0.267888314					
Total	36	249.994549						
	Coefficients	*Standard Error*	*t Stat*	*P-value*	*Lower 95%*	*Upper 95%*	*Lower 95.0%*	*Upper 95.0%*
Intercept	0	#N/A	#N/A	#N/A	#N/A	#N/A	#N/A	#N/A
S	0.554242429	0.048840795	11.3479403	9.41706E-13	0.454756985	0.653727873	0.454756985	0.653727873
L (m)	0.615676603	0.055183416	11.15691356	1.45757E-12	0.503271663	0.728081543	0.503271663	0.728081543
SxL	-0.105741471	0.010518749	-10.05266568	1.99339E-11	-0.127167462	-0.084315479	-0.127167462	-0.084315479
O	-2.587234702	0.387732986	-6.672722706	1.57157E-07	-3.37702095	-1.797448453	-3.37702095	-1.797448453

Table A3.3

The summary output for the multivariate-linear regression used to generate the formula for the Ψ_S factor that take in consider the common design practice in Palestine

SUMMARY OUTPUT								
Regression Statistics								
Multiple R	0.97355597							
R Square	0.947811227							
Adjusted R Square	0.911668529							
Standard Error	0.129434327							
Observations	36							
ANOVA								
	df	*SS*	*MS*	*F*	*Significance F*			
Regression	4	9.736293853	2.434073463	145.2896726	1.30626E-19			
Residual	32	0.536103836	0.016753245					
Total	36	10.27239769						
	Coefficients	*Standard Error*	*t Stat*	*P-value*	*Lower 95%*	*Upper 95%*	*Lower 95.0%*	*Upper 95.0%*
Intercept	0	#N/A	#N/A	#N/A	#N/A	#N/A	#N/A	#N/A
st num	0.080484427	0.012213927	6.589561947	1.992E-07	0.055605472	0.105363381	0.055605472	0.105363381
L (m)	0.083975916	0.013800066	6.085182172	8.48436E-07	0.055866101	0.112085731	0.055866101	0.112085731
stxl	-0.014758411	0.00263049	-5.610517396	3.36155E-06	-0.020116544	-0.009400278	-0.020116544	-0.009400278
or	0.220142811	0.096962841	2.270383249	0.030055186	0.022635966	0.417649656	0.022635966	0.417649656

Appendix B

Figures

Figure B1.1

Equivalent diagonal Compressive strut model represents infill panel in a frame

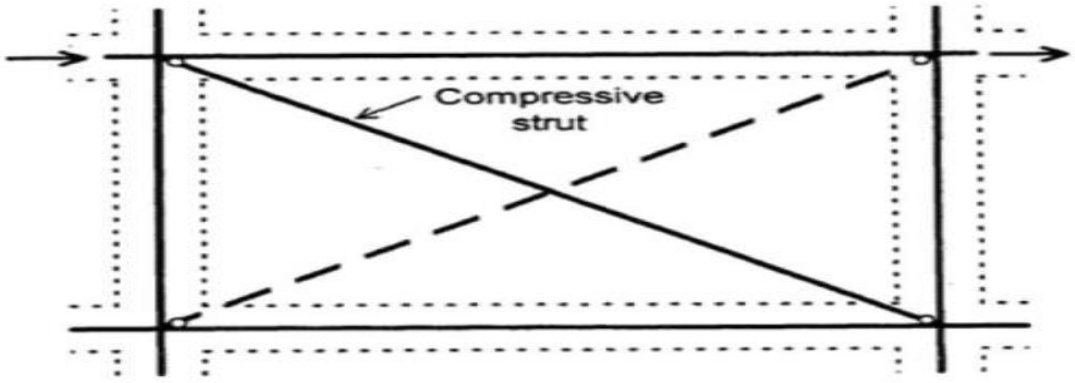

(Abdelkareem et- al, 2013).

Figure B1.2

Frame With Compression Struts That Represent Infill Walls

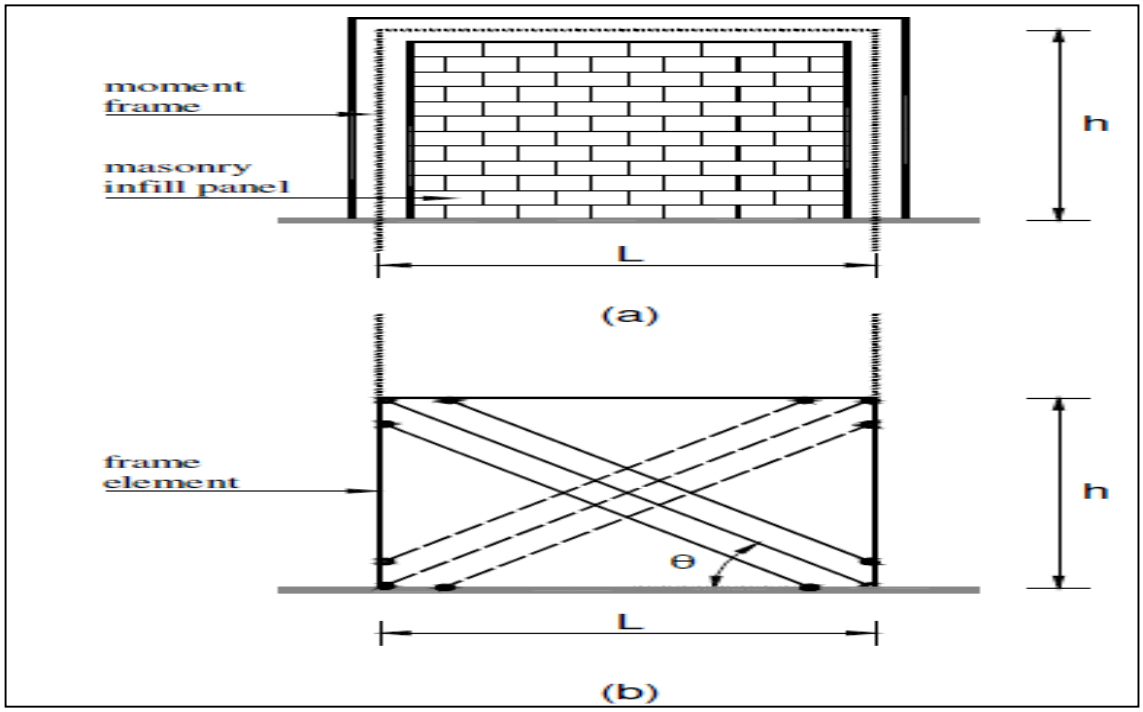

(Chrysostomou, 1991).

Figure B1.3

Parameters to estimate the diagonal strut width according to ASCE/SEI 41-06

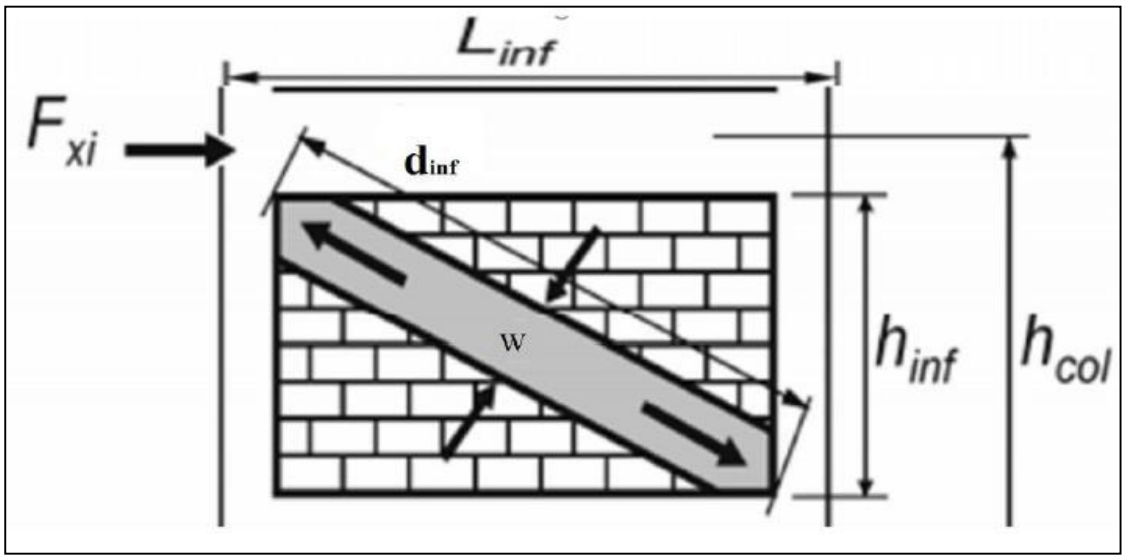

Figure B1.4

The variation of stiffness reduction factor for the frame having bay length L=4 m, column dimension b=h=40 cm, and window opening at center

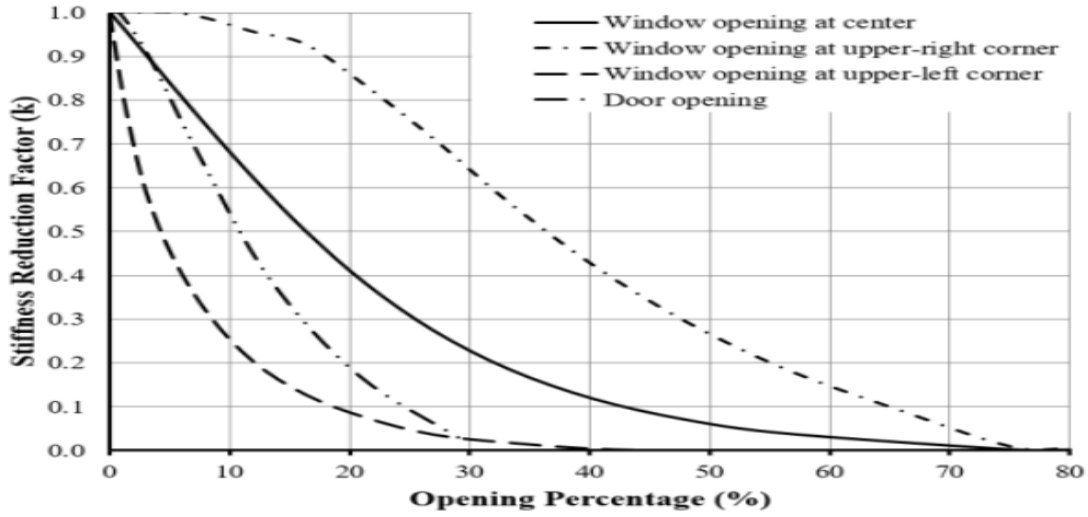

(a) L=4 m, b=h=40 cm

(Öztürkoğlu et al., 2017).

Figure B1.5

Comparison of strut width by Al-Hroub (2022)

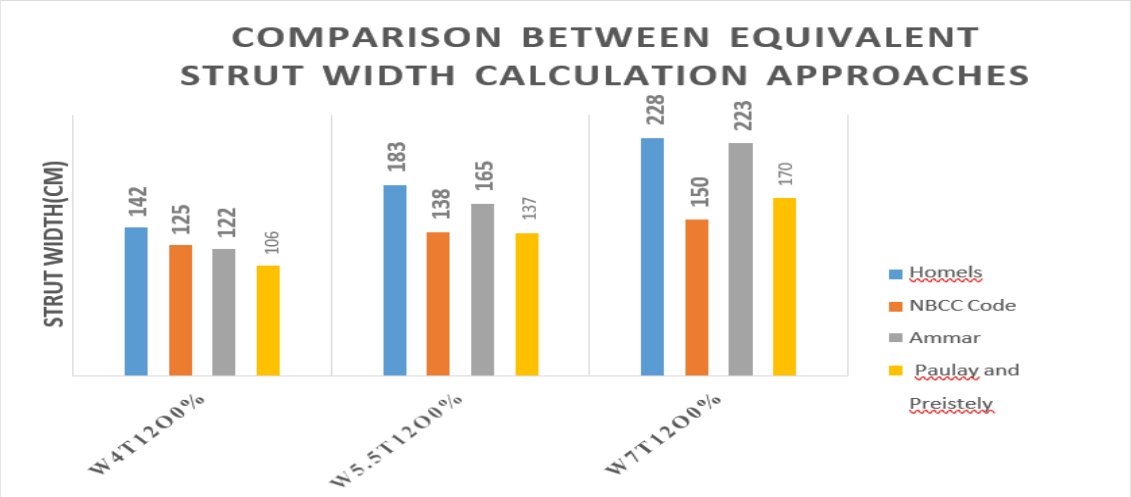

Figure B1.6

Stiffness reduction factor

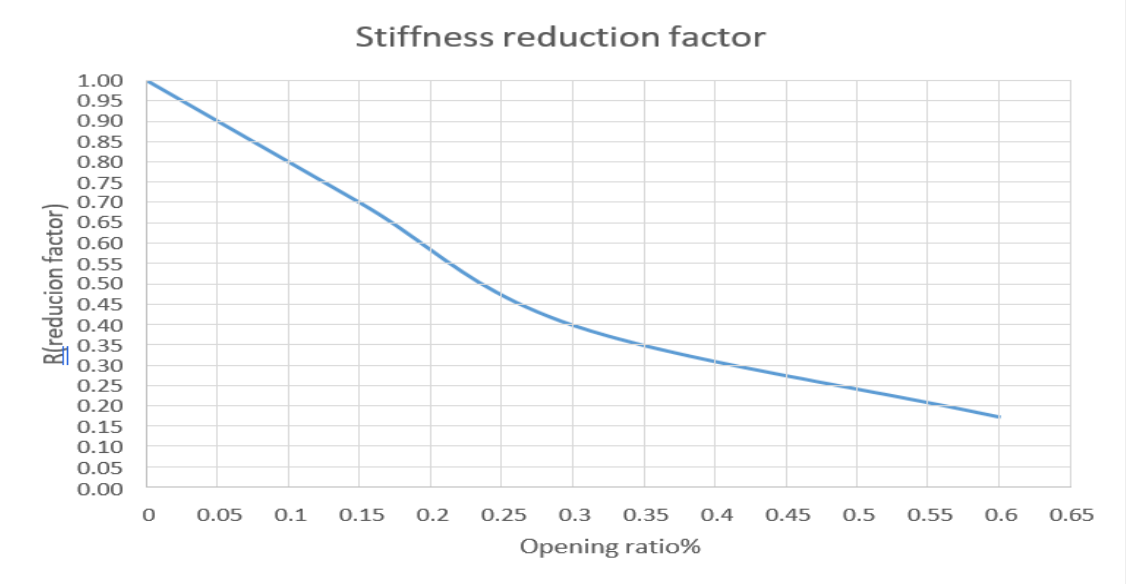

(Al-Hroub, 2022).

Figure B1.7

The backbone curve parameters

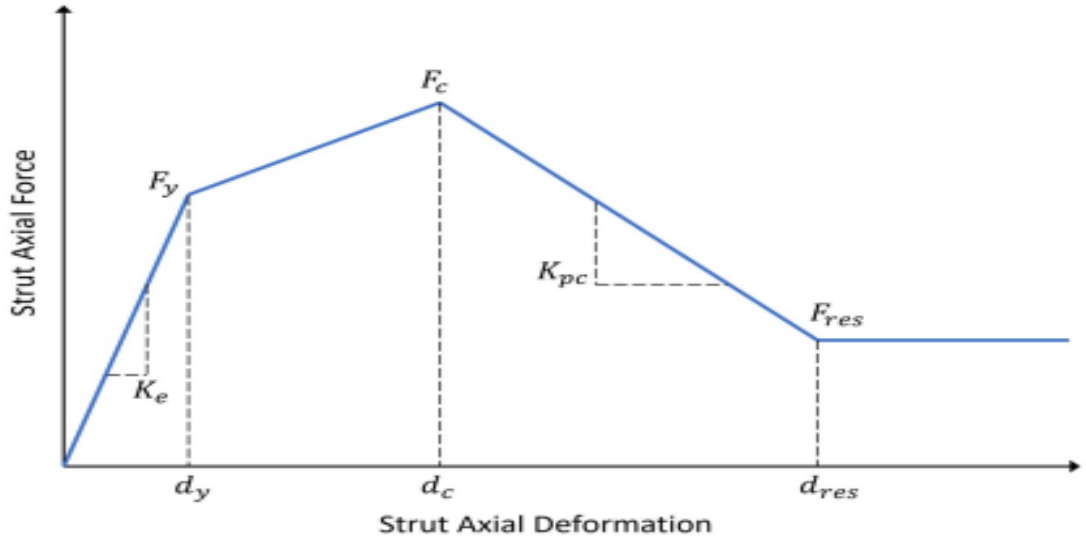

(Huang et al., 2020).

Figure B2.1

Force-deformation parameters for the equivalent compression strut

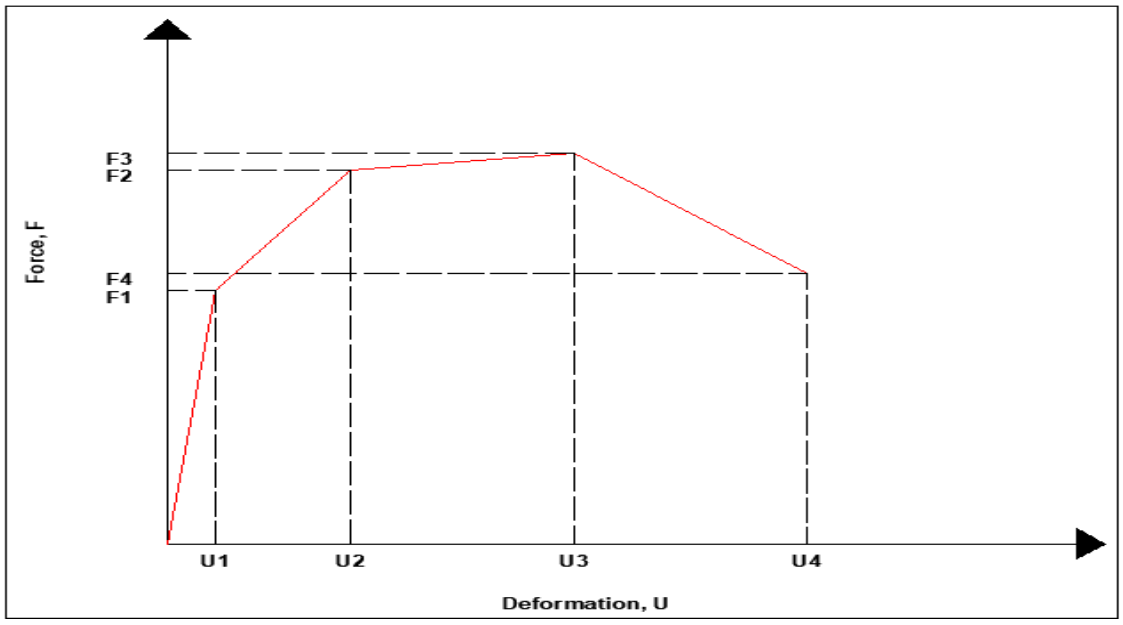

Figure B2.2

Example for the visual match for RC frame with BCSM infill wall with length of 5.5 m, and opening ratio of %30

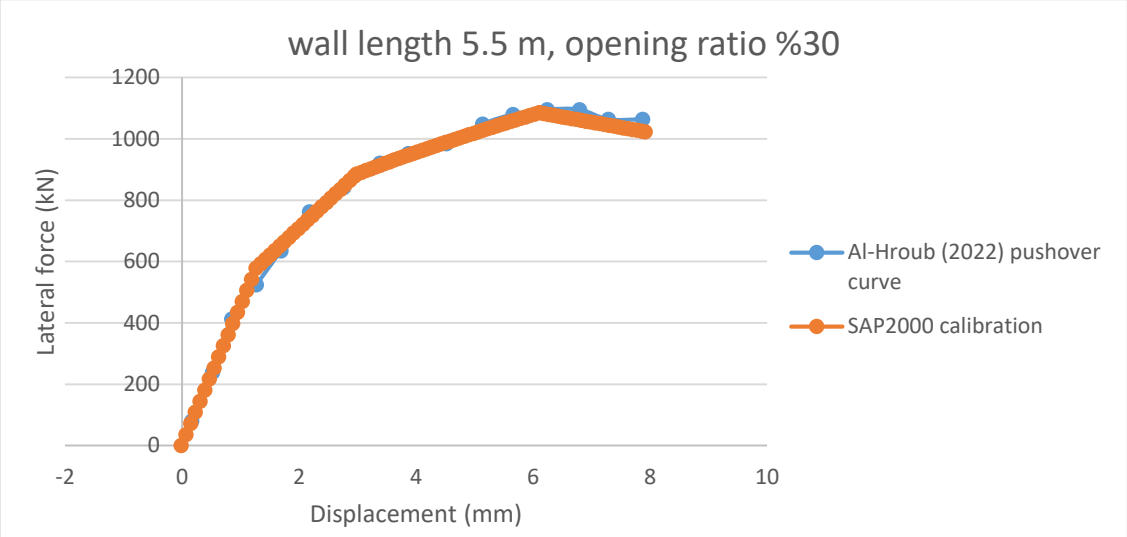

Figure B2.3

Reinforced concrete column section that has been drawn using the section designer

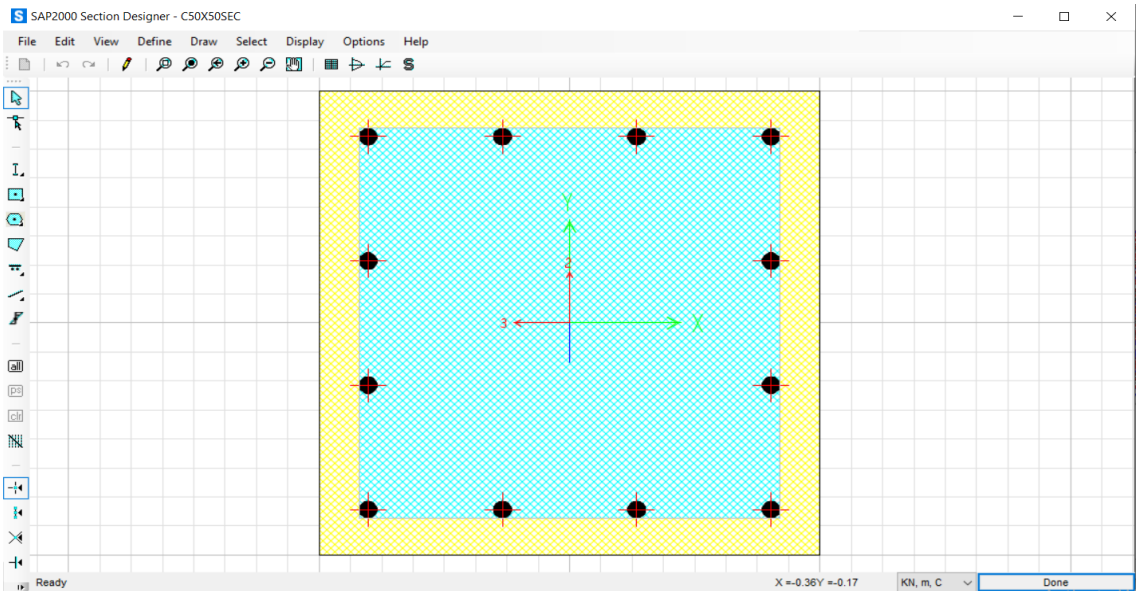

Figure B2.4

Stress-strain curve for the unconfined concrete of the column (column shown in Figure B2.3)

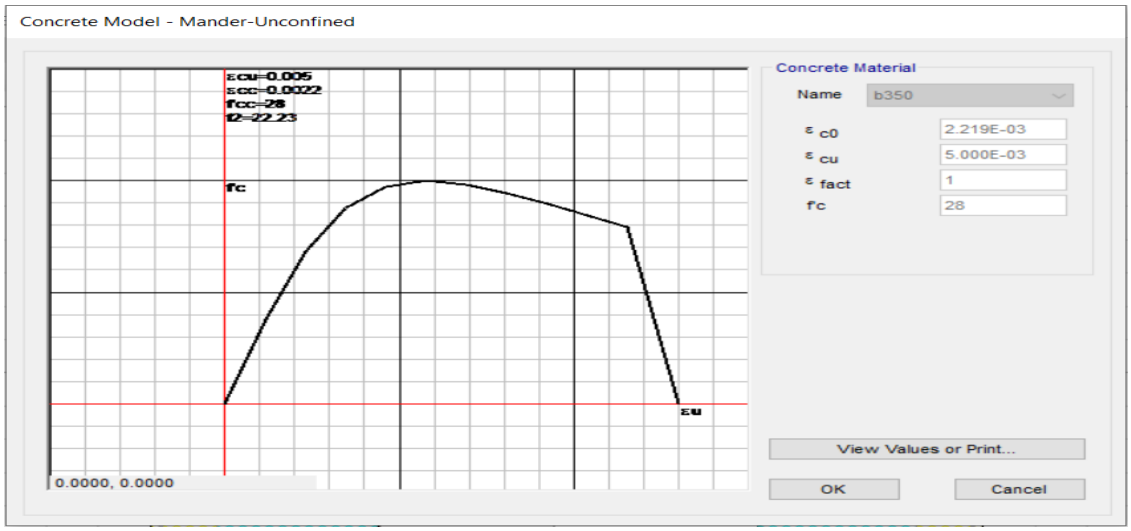

Figure B2.5

Stress-strain curve of the column (column shown in Figure B2.3)

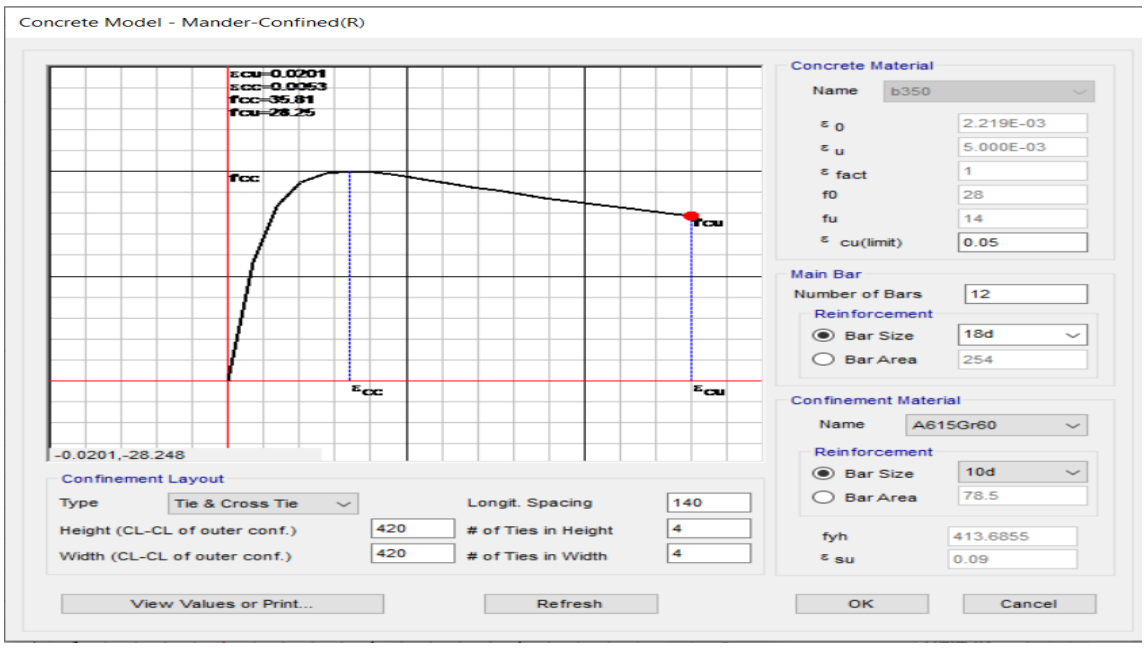

Figure B2.6

Stress-strain curve for the rebars of the column (column shown in Figure B2.3)

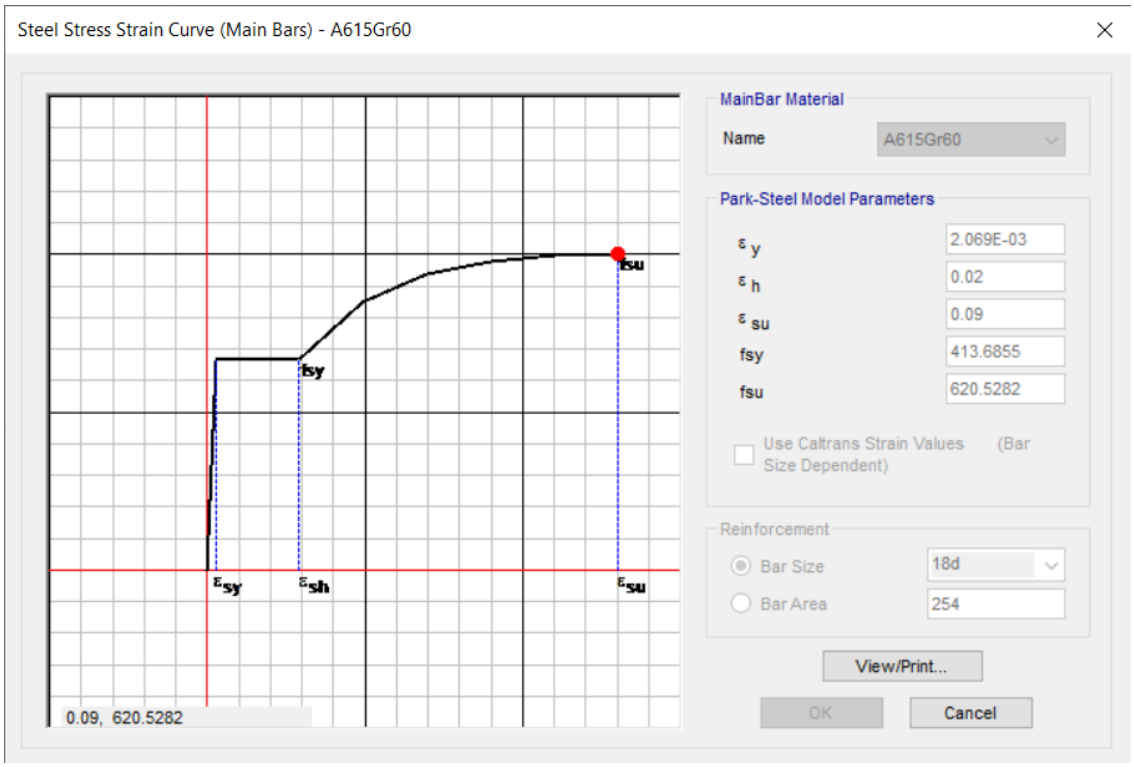

Figure B2.7

The 3D view of the building

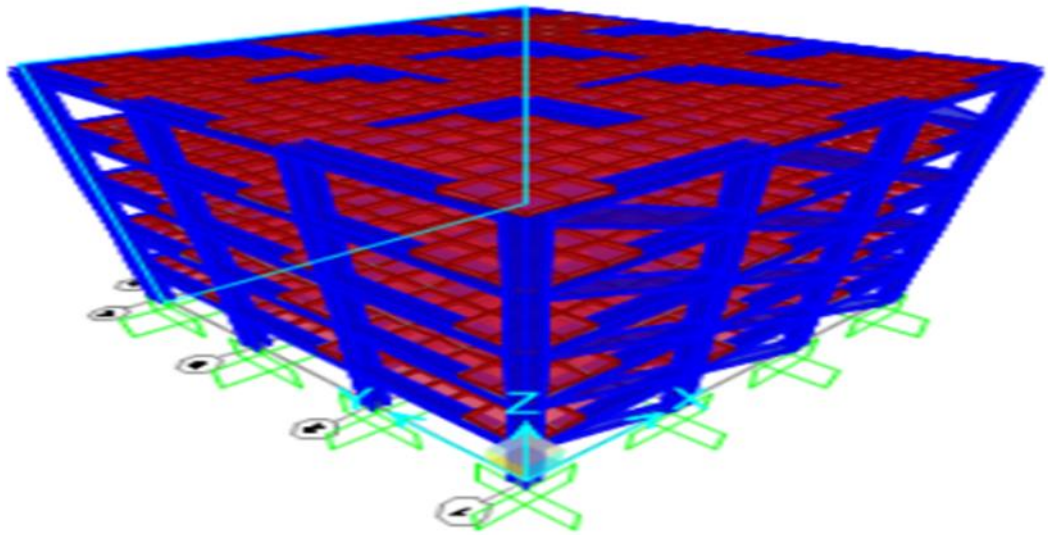

Figure B2.8

The 2D view of the building

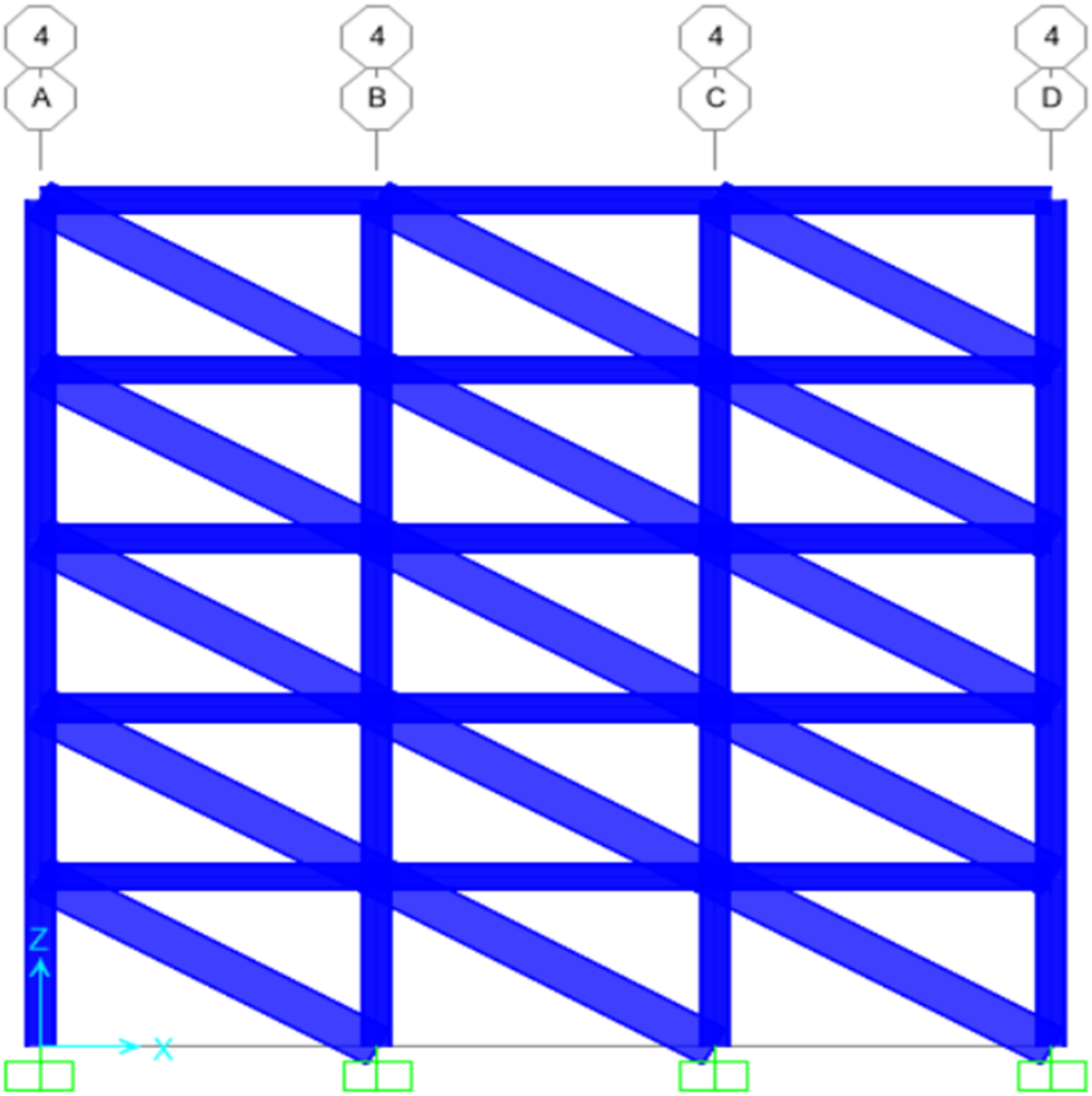

Figure B2.9

Columns grid

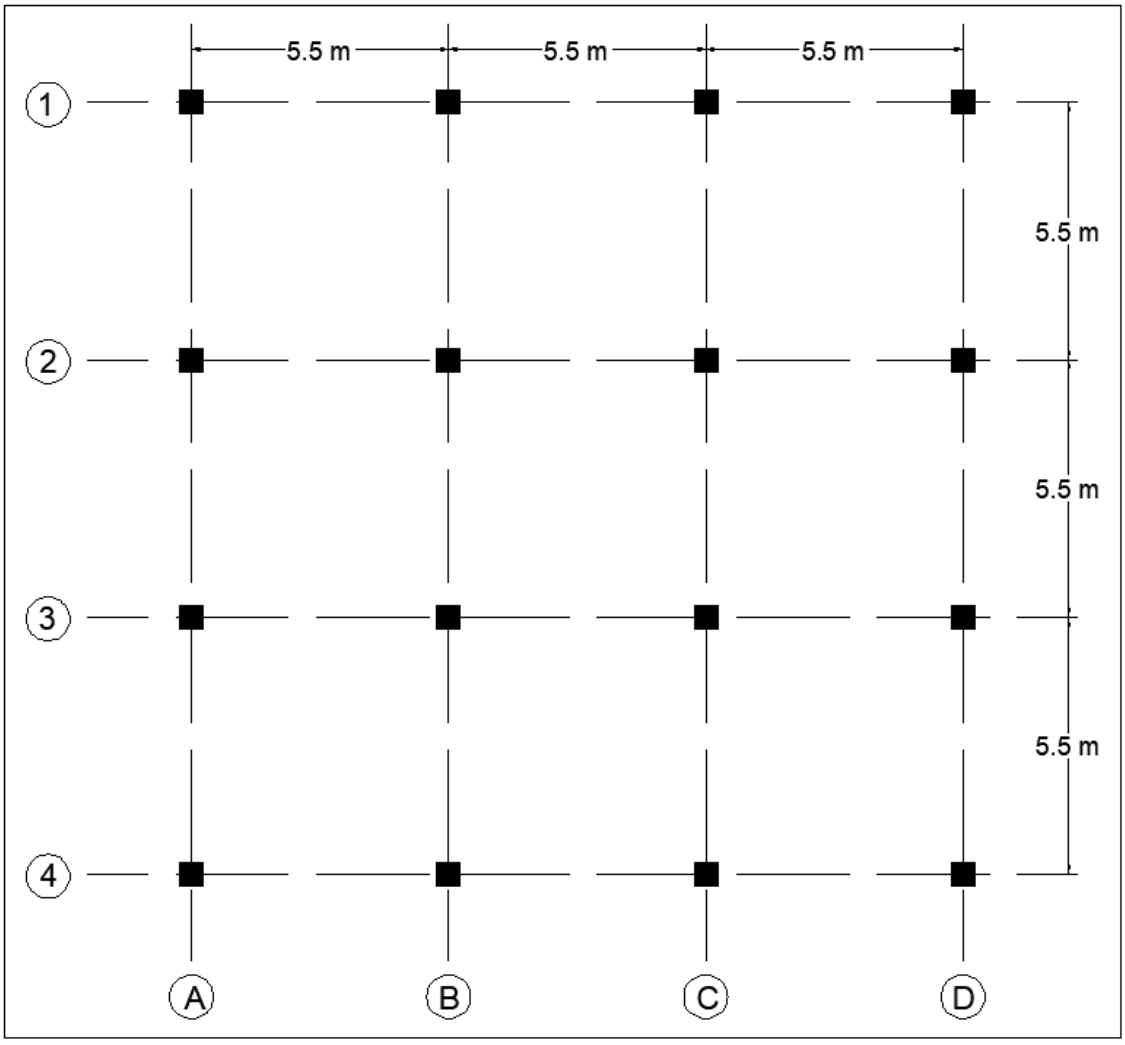

Figure B2.10

Hinge property data for beams and columns

Figure B2.11

The definition data of the fibers for the beams

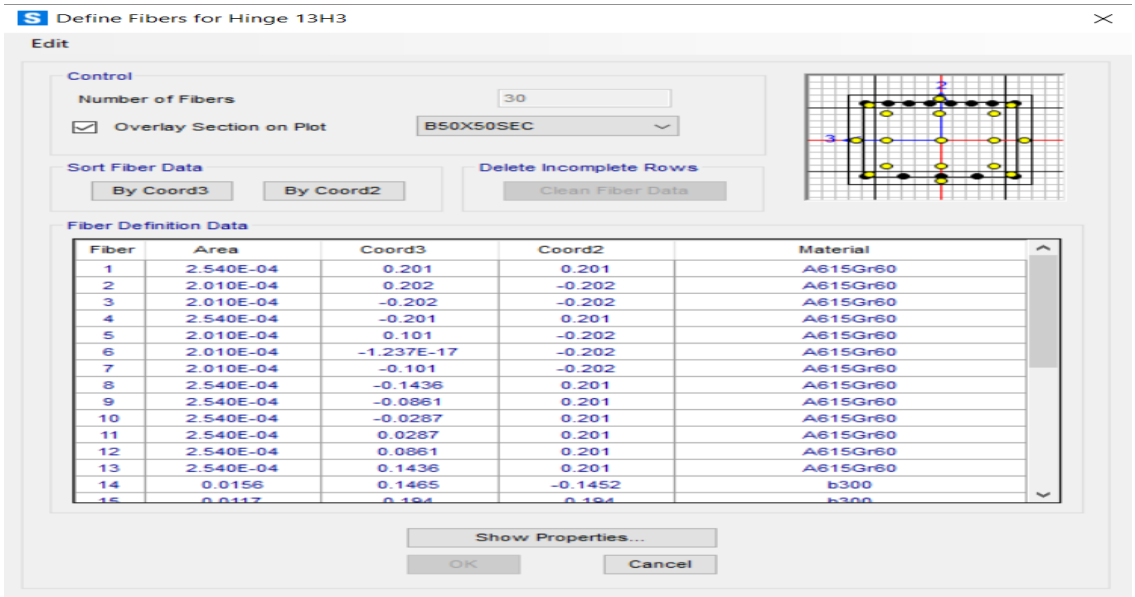

Fiber	Area	Coord3	Coord2	Material
1	2.540E-04	0.201	0.201	A615Gr60
2	2.010E-04	0.202	-0.202	A615Gr60
3	2.010E-04	-0.202	-0.202	A615Gr60
4	2.540E-04	-0.201	0.201	A615Gr60
5	2.010E-04	0.101	-0.202	A615Gr60
6	2.010E-04	-1.237E-17	-0.202	A615Gr60
7	2.010E-04	-0.101	-0.202	A615Gr60
8	2.540E-04	-0.1436	0.201	A615Gr60
9	2.540E-04	-0.0861	0.201	A615Gr60
10	2.540E-04	-0.0287	0.201	A615Gr60
11	2.540E-04	0.0287	0.201	A615Gr60
12	2.540E-04	0.0861	0.201	A615Gr60
13	2.540E-04	0.1436	0.201	A615Gr60
14	0.0156	0.1465	-0.1452	b300
15	0.0117	0.194	0.194	b300

Figure B2.12

The definition data of the fibers for the columns

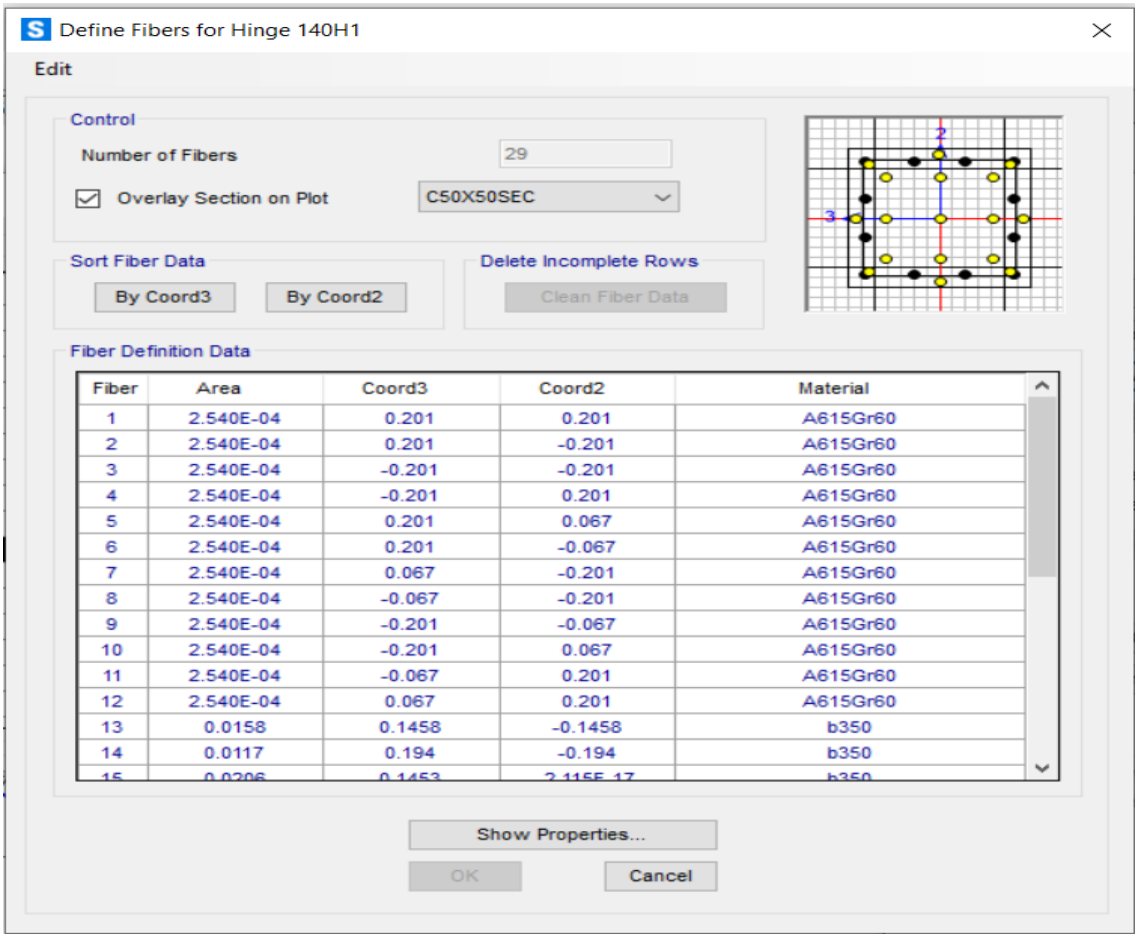

Fiber	Area	Coord3	Coord2	Material
1	2.540E-04	0.201	0.201	A615Gr60
2	2.540E-04	0.201	-0.201	A615Gr60
3	2.540E-04	-0.201	-0.201	A615Gr60
4	2.540E-04	-0.201	0.201	A615Gr60
5	2.540E-04	0.201	0.067	A615Gr60
6	2.540E-04	0.201	-0.067	A615Gr60
7	2.540E-04	0.067	-0.201	A615Gr60
8	2.540E-04	-0.067	-0.201	A615Gr60
9	2.540E-04	-0.201	-0.067	A615Gr60
10	2.540E-04	-0.201	0.067	A615Gr60
11	2.540E-04	-0.067	0.201	A615Gr60
12	2.540E-04	0.067	0.201	A615Gr60
13	0.0158	0.1458	-0.1458	b350
14	0.0117	0.194	-0.194	b350
15	0.0206	0.1453	-2.115E-17	b350

Figure B2.13

The axial plastic hinge definition for the equivalent compression strut

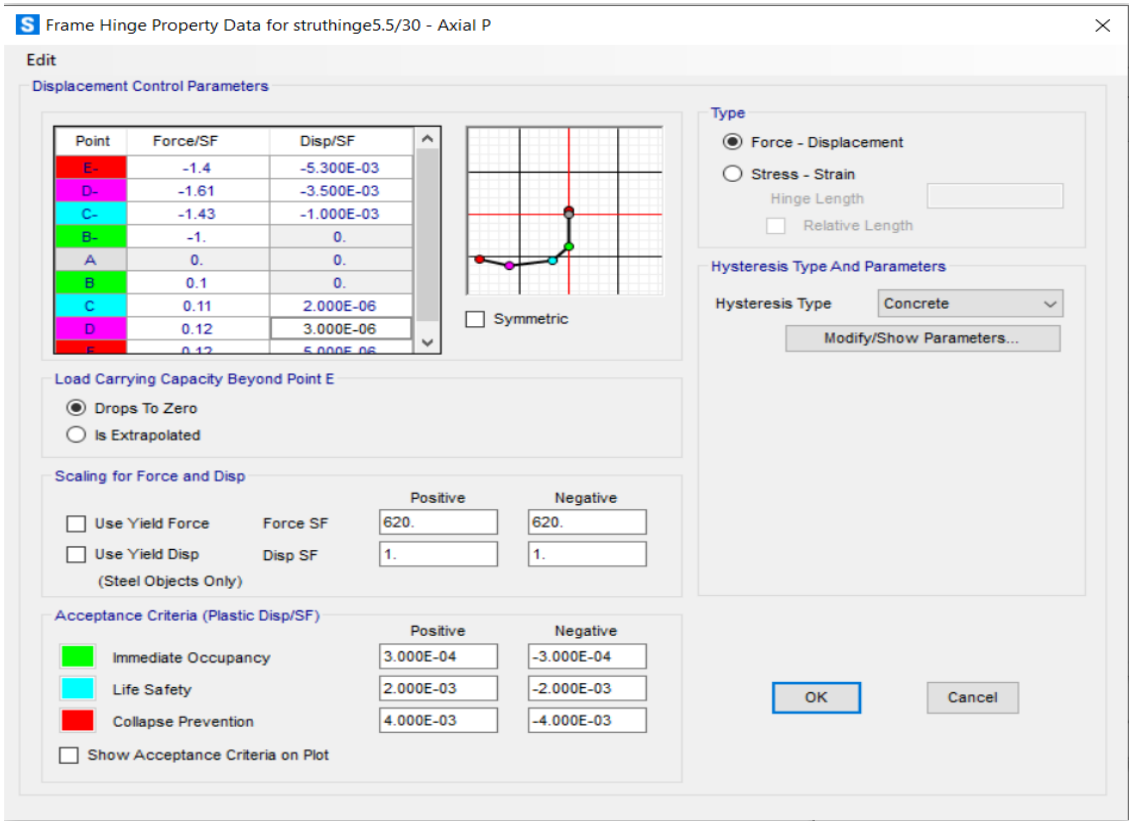

Figure B2.14

The assumed plastic hinge length for beams and columns

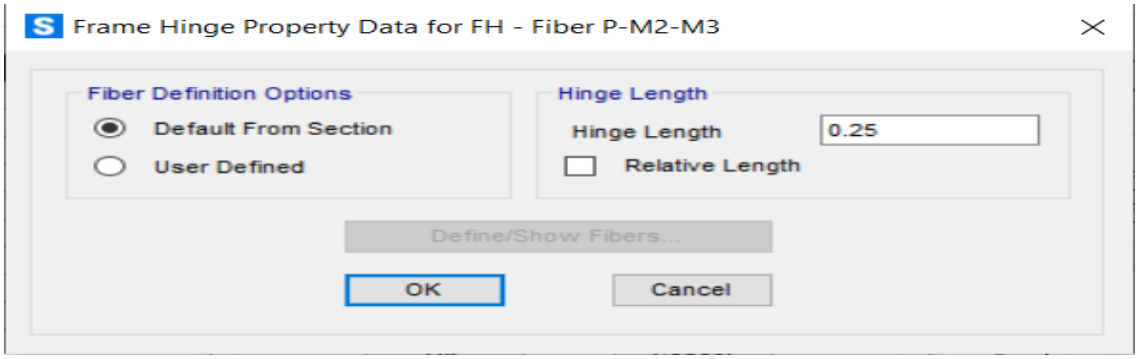

Figure B2.15

The gravity load case definition

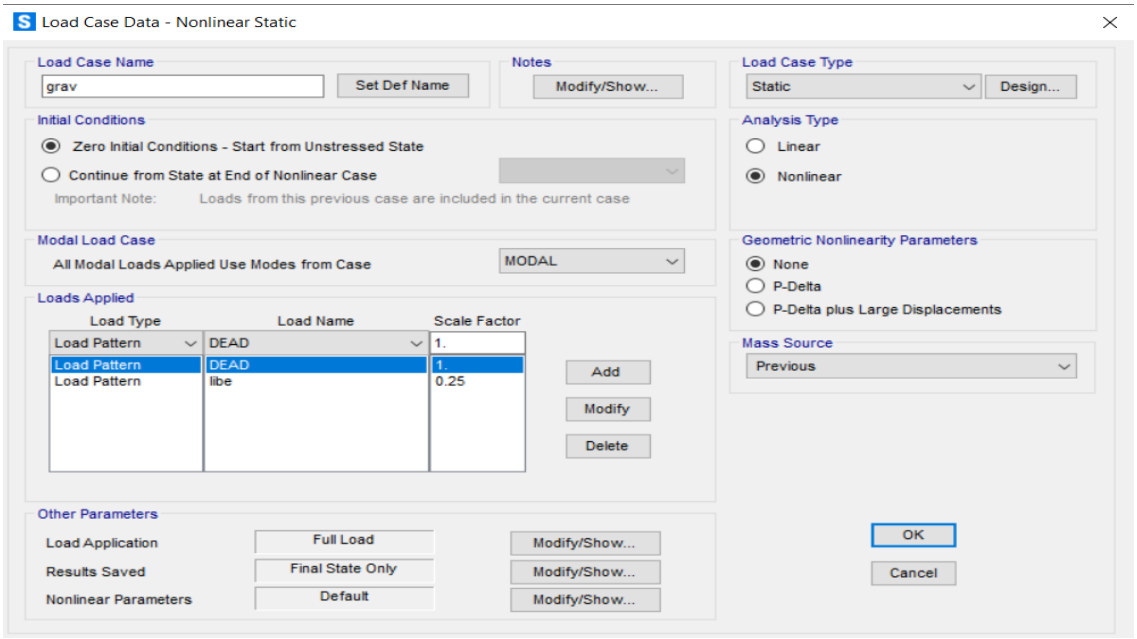

Figure B2.16

The pushover load case definition

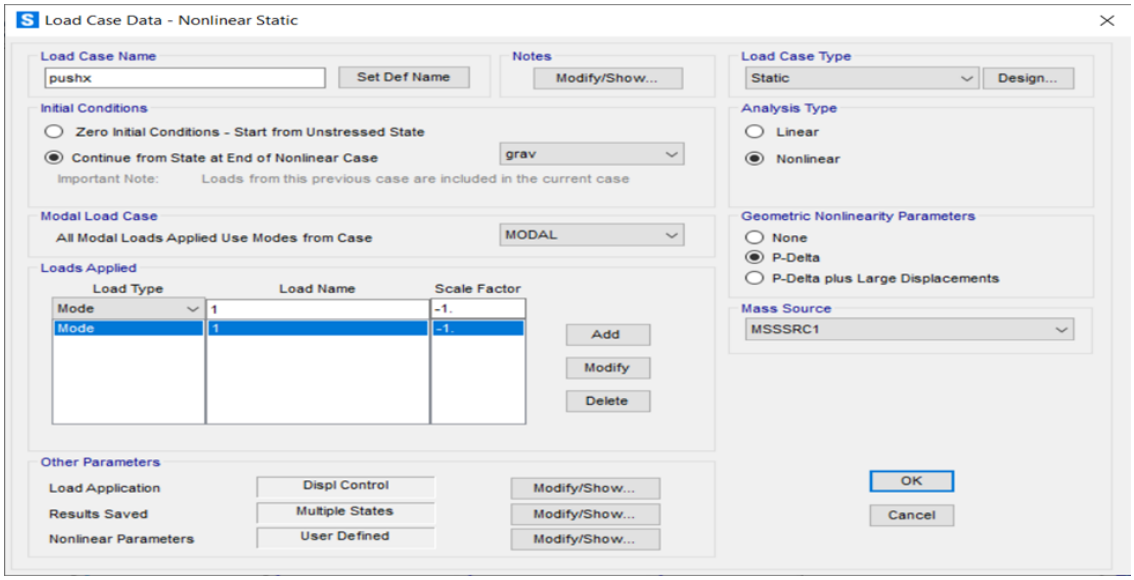

Figure B2.17

The reinforcement detailing and the geometrical properties of the RC frame (Cavaleri et al., 2004)

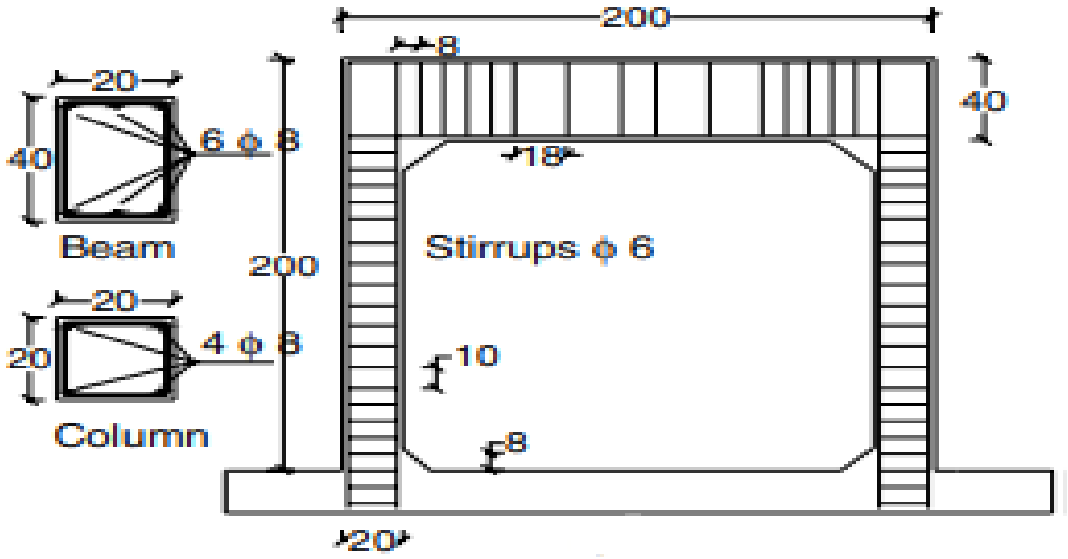

Figure B2.18

The bending moments on the frame elements due to 1-unit load

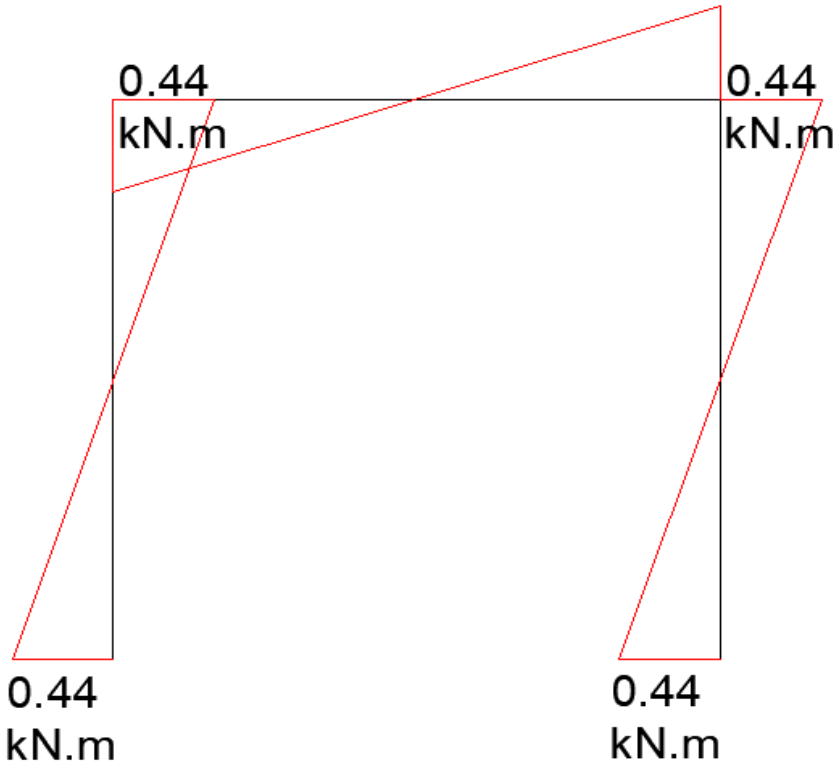

Figure B2.19

The curvature of the frame elements when the columns reach yielding

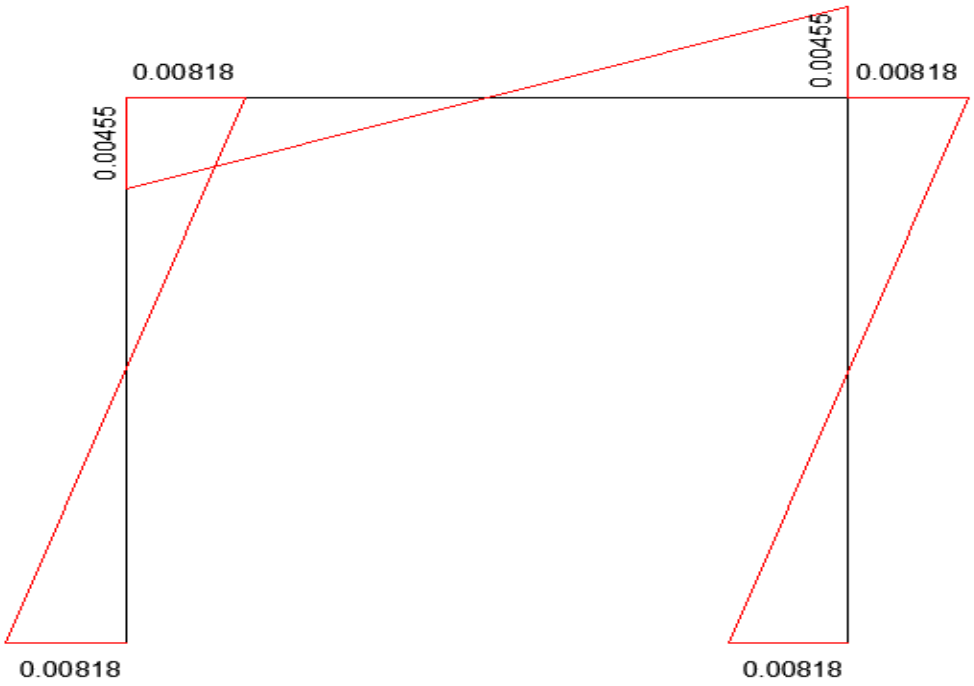

Figure B2.20

Comparison between the pushover curves for experiment, SAP 2000, and manual pushover curves

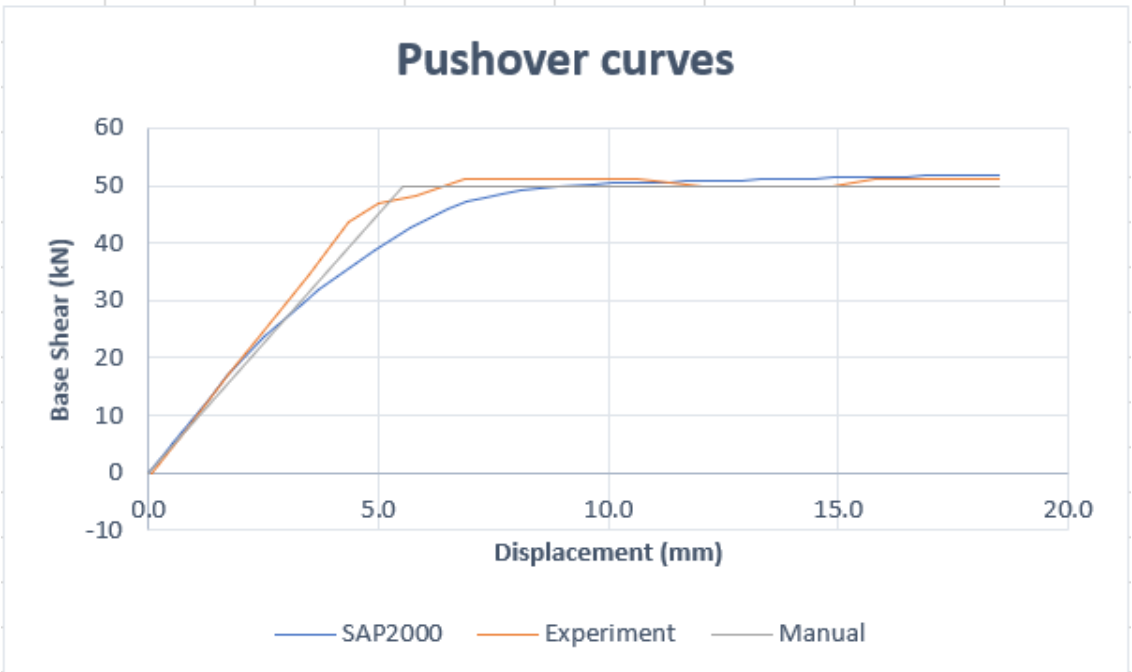

Figure B2.21

Comparison between pushover curves for Al-Hroub (2022) micro model and SAP 2000 pushover curves

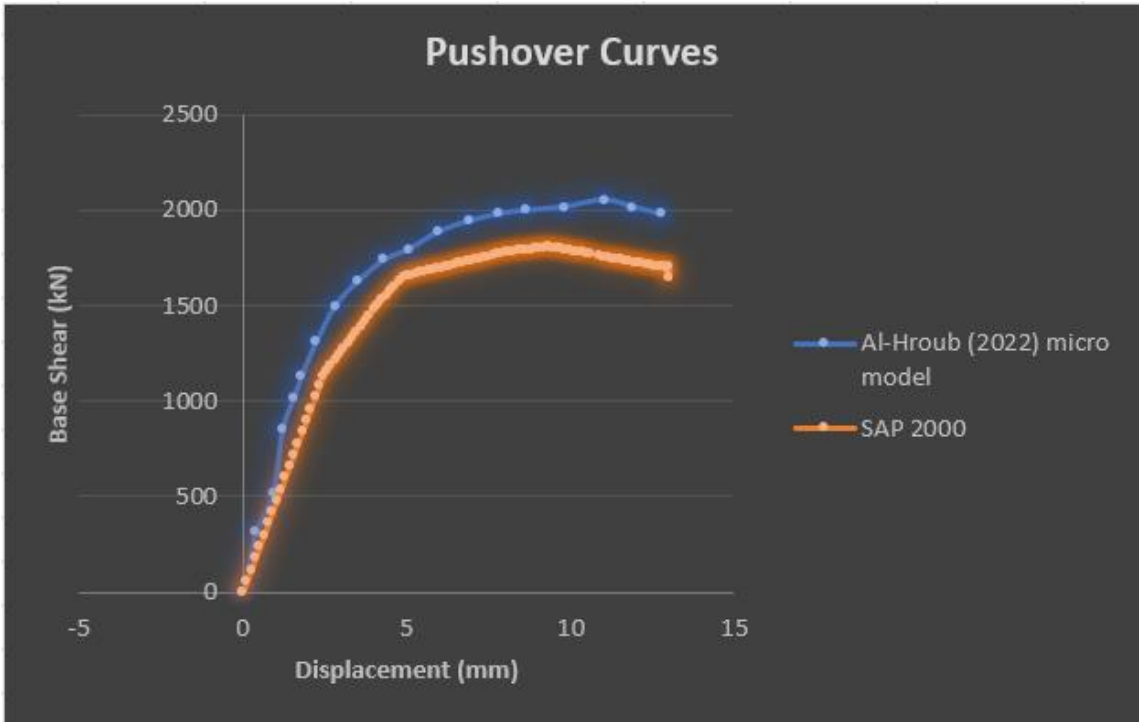

Figure B3.1

The performance of the elements for S11L7O60 model at roof displacement where maximum base shear occurs

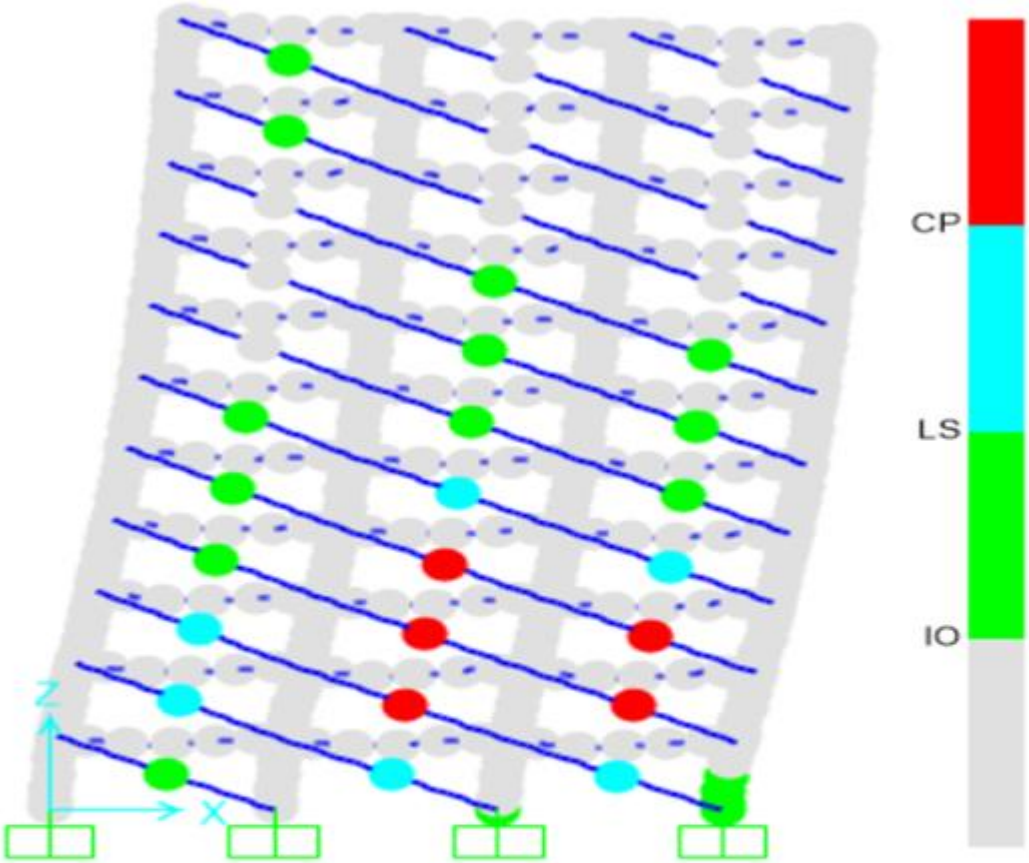

Where:

IO: represent the immediate occupancy performance.

LS: represent the life safety performance.

CP: represent the collapse prevention performance.

Figure B3.2

The performance of the elements for S11L7O100 model at roof displacement where maximum base shear occurs

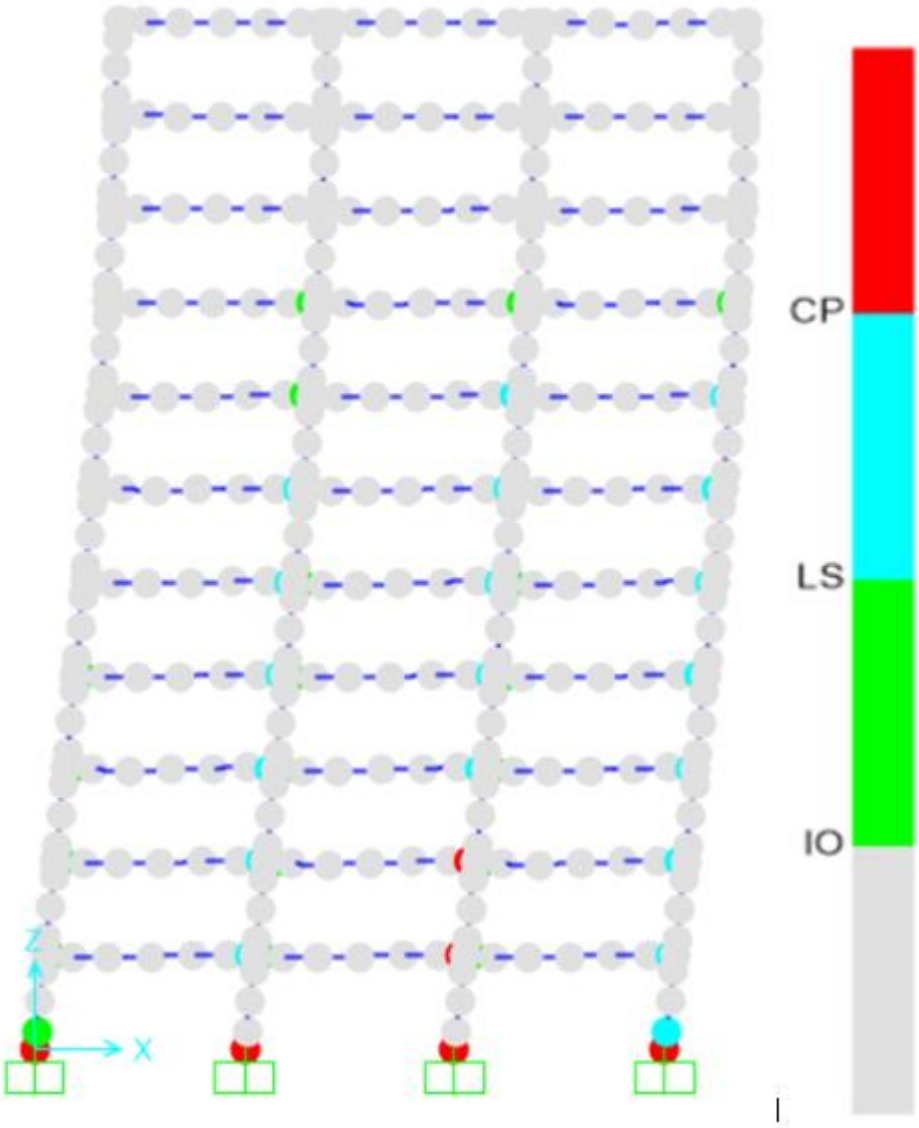

Figure B3.3

The performance of the elements for S5L7O60 model at roof displacement where maximum base shear occurs

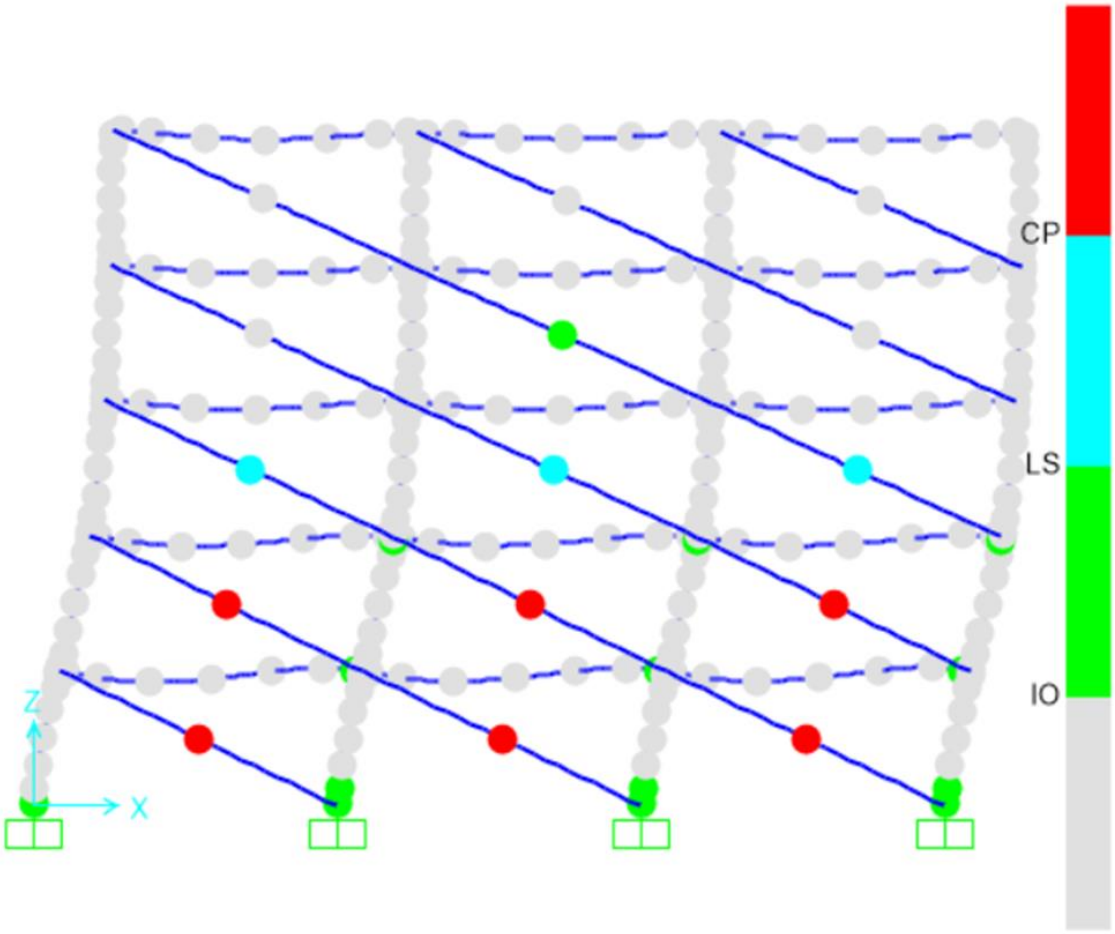

Figure B3.4

The performance of the elements for S5L7O100 model at roof displacement where maximum base shear occurs

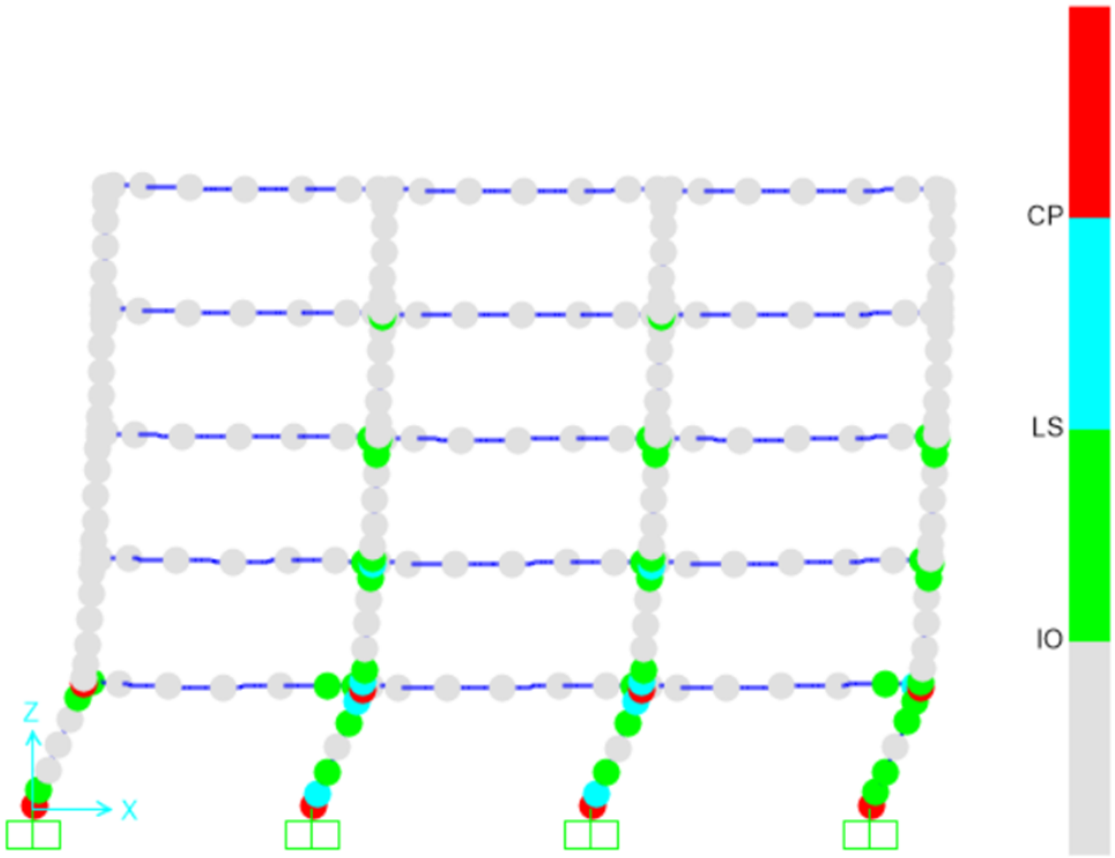

Figure B3.5

Pushover curves for bare building models

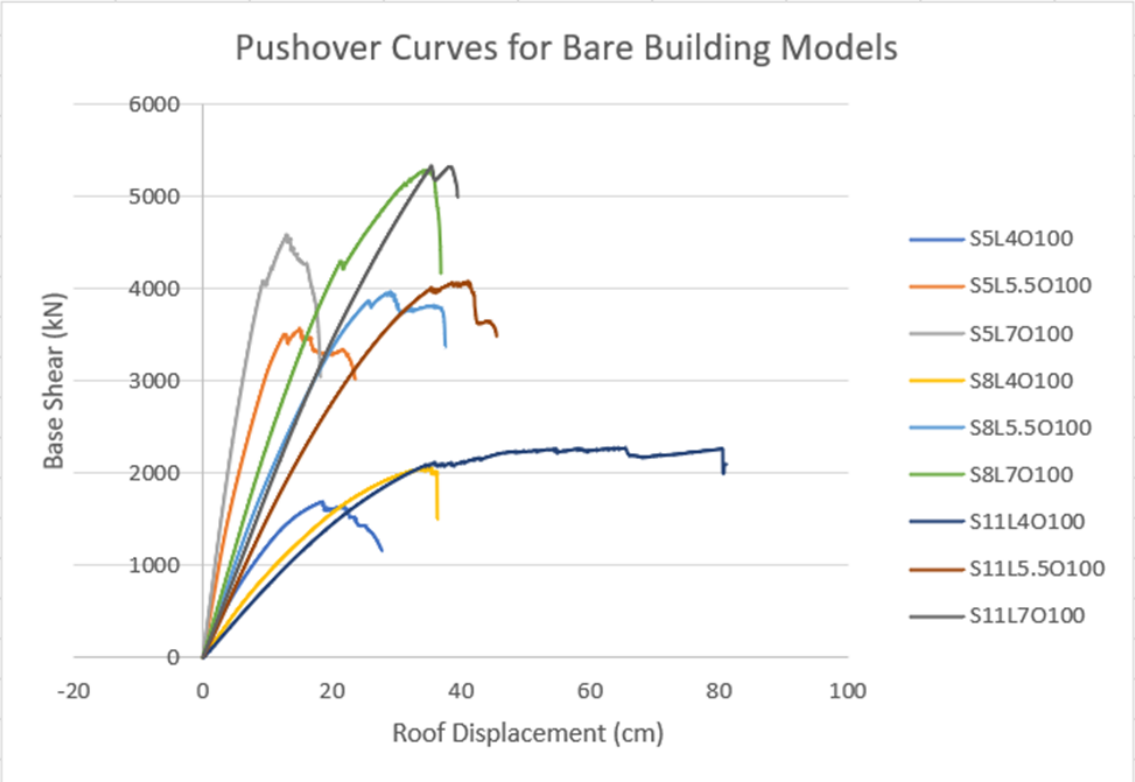

Figure B3.6

Variation of the overstrength factor for building models with 5 stories, 8 stories, and 11 stories and with frames span length of 5.5 m under the variation of the opening ratio of the BCSM infill wall

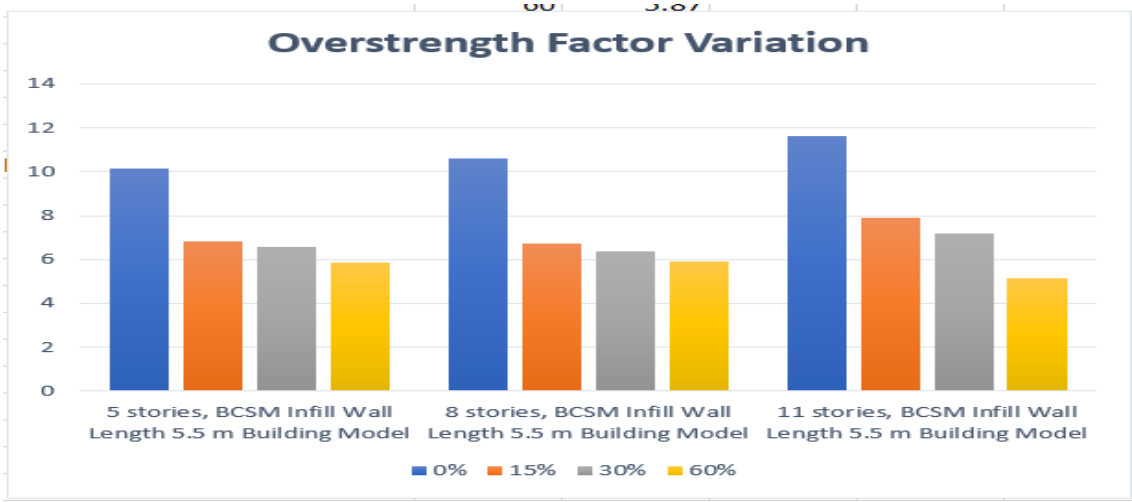

Figure B3.7

The residuals for each term in the Ψ_S factor formula

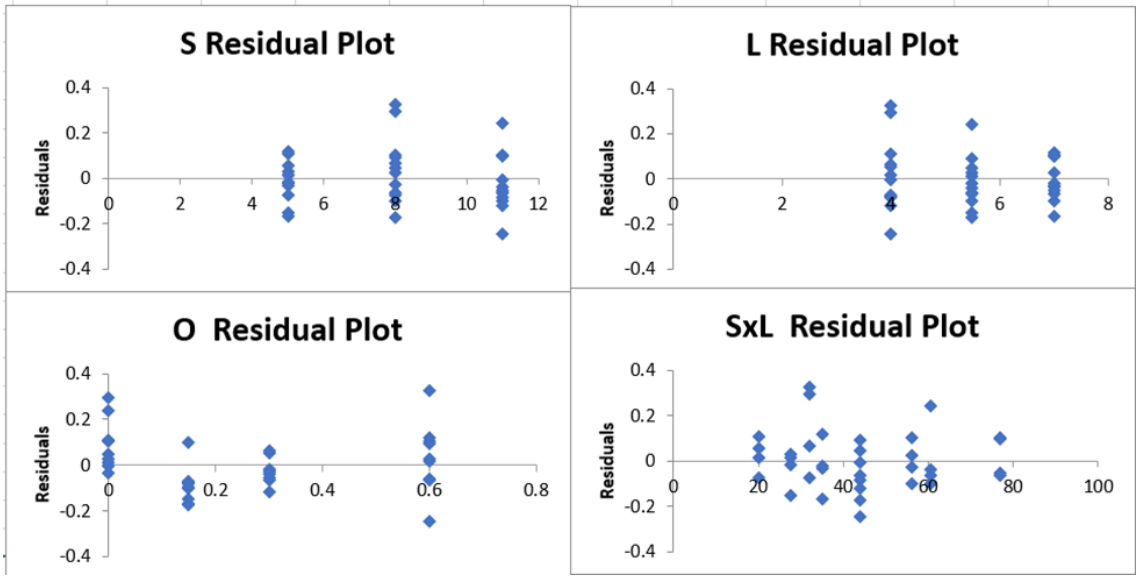

Figure B3.8

Pushover curves for the 6 building models

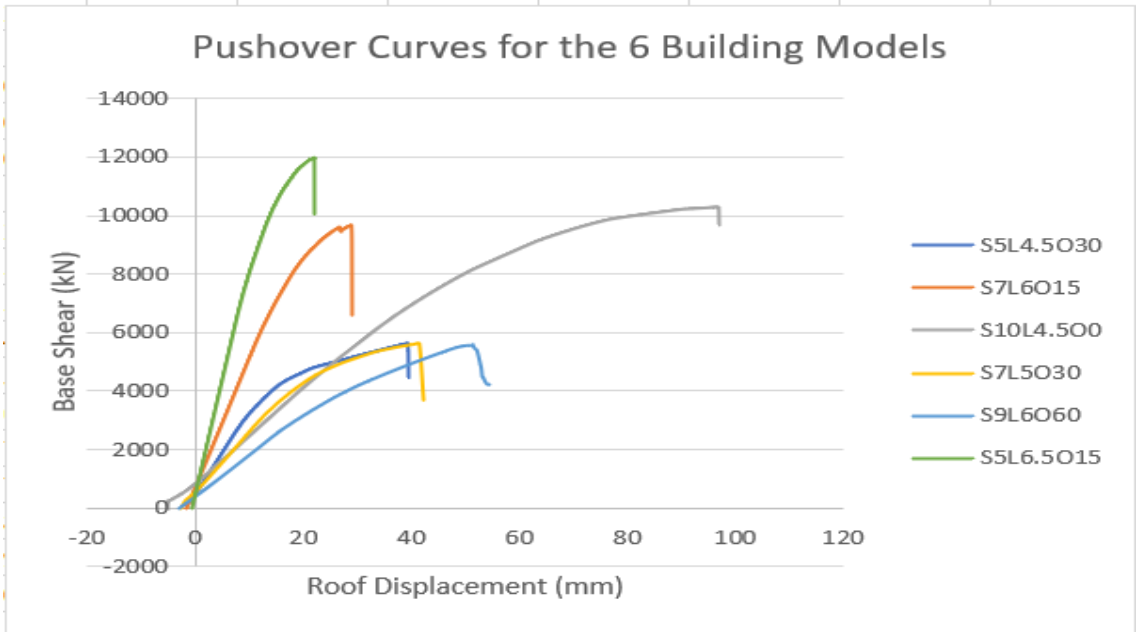

جـامعـــة النجاح الوطنية
كليـــة الدراســـات العليـــا

أثر الجدران الحجرية الخارجية المكونة من طوب وخرسانة وحجر على معامل تضخيم الإزاحة للإطارات المتوسطة

إعداد
خالد جمال مصاروه

إشراف
د. منذر دويكات
د. محمد سماعنة

قدمت هذه الأطروحة استكمالا لمتطلبات الحصول على درجة الماجستير في هندسة الإنشاءات، من كلية الدراسات العليا، في جامعة النجاح الوطنية، نابلس –فلسطين.

2024

أثر الجدران الحجرية الخارجية المكونة من طوب وخرسانة وحجر على معامل تضخيم الإزاحة للإطارات المتوسطة

إعداد
خالد جمال مصاروه
إشراف
د. منذر دويكات
د. محمد سماعنة

الملخص

يعد تشييد المباني متعددة الطوابق والتي تحتوي على جدران خارجية مكسوة بالحجر أمرًا شائعًا جدًا في فلسطين؛ حيث تضفي الكسوة الحجرية جمالية معمارية على الواجهات الخارجية للمباني. الطريقة التقليدية في فلسطين لبناء هذه الجدران هي ملء الإطارات الخرسانية المسلحة بجدار ثلاثي الطبقات. وهذه الطبقات هي: الطوب، والخرسانة، والحجر. قد تؤثر هذه الجدران على سلوك المنشأ تحت الحركة الزلزالية ويرجع ذلك إلى كتلتها الثقيلة المركزة الإضافية، وصلابتها الجانبية الإضافية، وقوتها الجانبية الإضافية التي تضيفها هذه الجدران إلى المبنى. إن إهمال تأثير هذه الجدران على الاستجابة الإنشائية يمكن أن يؤدي إلى سوء التنبؤ بين نتائج التحليل الإنشائي والسلوك الإنشائي الحقيقي. لذلك، تركز هذه الدراسة على دراسة تأثير الجدران الحجرية الخارجية المكونة من طوب وخرسانة وحجر على معامل تضخيم الإزاحة للإطارات المتوسطة.

بدأت منهجية البحث بتصميم 36 نموذج بناء حسب الكود ASCE7-16 وACI 318-14، وتم تصميم كل نموذج بناء كإطار متوسط. بعد تصميم جميع نماذج البناء الـ 36، تم تعريف المفصلات اللدنة وتخصيصها لكل عضو في كل نموذج بناء. تم إجراء تحليل الدفع الساكن غير الخطي لتوليد منحنيات حمل مع إزاحة لعدة سيناريوهات من المتغيرات باستخدام برنامج SAP200. تم استخدام هذه المنحنيات لتقدير معامل تضخيم الإزاحة تحت تنوع المتغيرات.

أظهرت النتائج أن زيادة نسبة الفتحة في الجدران المكونة من طوب وخرسانة وحجر تؤدي إلى نقص في قيمة معامل تضخيم الإزاحة. كما وأظهرت النتائج أن زيادة طول الجدران المكونة من طوب وخرسانة وحجر تؤدي إلى نقص في قيمة معامل تضخيم الإزاحة. وأخيراً ، أظهرالنتائج أن تأثير عدد طوابق المبنى على معامل تضخيم الإزاحة ليس ثابتاً دائماً؛ بمعنى آخر، ليس صحيحاً أن زيادة عدد طوابق المبنى ستؤدي دائماً إالى زيادة قيمة معامل تضخيم الإزاحة والعكس صحيح.

ختاماً، تم إستنتاج أن قيمة معامل تضخيم الإزاحة حساسة جداً لوجود الجدران المكونة من طوب وخرسانة وحجر؛ حيث يمكن أن تؤدي هذه الجدران إلى تغير كبير في قيمة معامل تضخيم الإزاحة والتي قد تصل إلى أربعة أضعاف مقارنة مع ما هو موجود في كود ال ASCE7-16.

تم استخدام النتائج لإيجاد معادلتين بسيطتين لحساب قيمة معامل تضخيم الإزاحة ؛ أحد هذه المعادلات لحساب قيمة معامل تضخيم الإزاحة بشكل عام، والمعادلة الأخرى لمساعدة المهندسين في فلسطين على الاستفادة من وجود الجدران المكونة من طوب وخرسانة وحجر؛ حيث أن ممارسة التصميم الشائعة في فلسطين تأخذ فقط تأثير هذه الجدران من حيث الكتلة والوزن في عملية التصميم وتهمل تأثير هذه الجدران في إضافتها للصلابة والقوة الجانبية للمبنى.

الكلمات المفتاحية: الجدران المكونة من طوب وخرسانة وحجر، النماذج الكبيرة، التحليل اللاخطي، المفاصل اللدنة، معامل تضخيم الإزاحة، معامل تعديل الإستجابة، دعامة الضغط المكافئة.